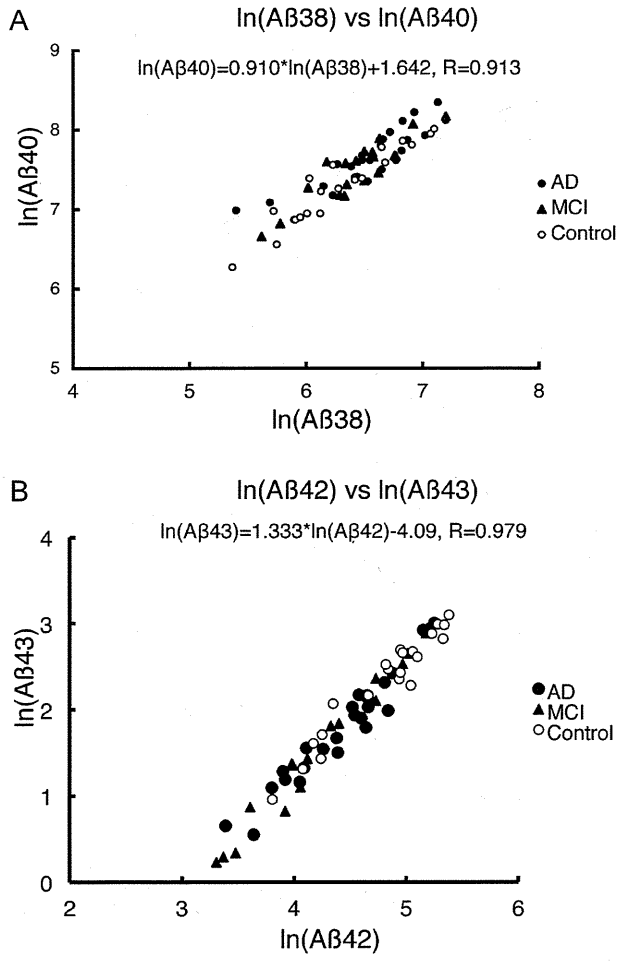

Figure 2. Relationships between the levels of Aβ40 and 38, and between those of Aβ43 and 42 in CSF from controls and MCI/AD patients.

A. The levels of ln(Aβ40) were proportional to those of ln(Aβ38) ($\ln(A\beta40) = 0.910 \times \ln(A\beta38) + 1.642$, $R = 0.913$).

B. The levels of ln(Aβ43) were proportional to those of ln(Aβ42) ($\ln(A\beta43) = 1.333 \times \ln(A\beta42) - 4.09$, $R = 0.979$). It should be noted that the levels of both ln(Aβ42) and ln(Aβ43) in MCI [filled triangle ($n = 19$)]/AD [filled circle ($n = 24$)] are lower than those in controls [open circles ($n = 21$)].

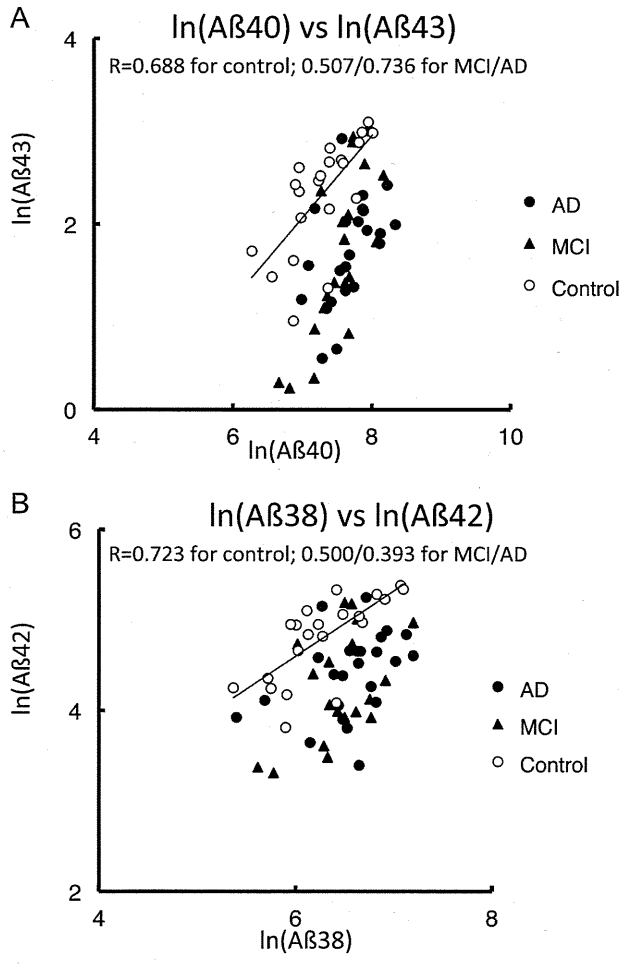

Figure 3. Relationships between the levels of Aβ43 and 40, and between those of Aβ42 and 38 in CSF from controls (open circles) and MCI (closed triangle)/AD patients (closed circle).

A. The levels of ln(Aβ43) correlate with those of ln(Aβ40) within controls ($R = 0.688$), and barely within MCI/AD subjects ($R = 0.507/0.736$). The plots for MCI/AD were located below the regression line for control ($p < 0.001$, ANOVA).

B. The levels of Aβ42 correlate with those of Aβ38 within controls ($R = 0.723$), and barely within MCI/AD ($R = 0.500/0.393$). The plots for MCI/AD were situated below the regression line for controls ($p < 0.001$, ANOVA).

concentrations of Aβ40 were significantly increased in AD compared to control (Table 1; $p < 0.05$, Dunnett's t-test). Additionally, the CSF concentrations of Aβ38 tended to be increased in AD patients compared to controls. In contrast, those of Aβ42 and 43 were significantly decreased in MCI/AD compared to controls ($p < 0.05$, Dunnett's t-test). Interestingly, as reported previously (Schoonenboom et al, 2005), the CSF concentrations of Aβ40 and Aβ38 were proportional to each other in all subjects [Fig 2A; $\ln(A\beta40) = 0.910 \times \ln(A\beta38) + 1.642$, $R = 0.913$, where ln(Aβ40) is the logarithm of Aβ40], even in MCI/AD cases. This was despite the fact that these species are derived from and the final products of the two different product lines of γ-secretase activity (Fig 1; Takami et al, 2009). In other words, the amounts of products in the third step of cleavage were strictly proportional to each other across the product lines.

Aβ42 and Aβ43 are produced by the second cleavage step of each product line. Like Aβ40 and Aβ38, the CSF concentrations of Aβ42 and Aβ43 are also proportional to each other in controls and in MCI/AD patients [Fig 2B; $\ln(A\beta43) = 1.333 \times \ln(A\beta42) - 4.09$, $R = 0.979$]. On the other hand, the levels of Aβ43 and Aβ40 (a precursor and its product) were correlated in control [Fig 3A; $\ln(A\beta43) = 0.884 \times \ln(A\beta40) - 4.118$, $R = 0.688$] and in MCI/AD subjects ($R = 0.507/0.736$ for MCI/AD, respectively) but the MCI/AD values were located below the regression line for controls and thus provided lower Aβ43 measures compared with controls for a given Aβ40 measure (Fig 3A; $p < 0.001$, analysis of variance, ANOVA). Conversely,

for a given Aβ43 value, the plot provided a higher Aβ40 measure in MCI/AD cases. There was a similar situation for the levels of Aβ42 and Aβ38. The levels of Aβ42 and Aβ38 were correlated each other in control subjects [Fig 3B; $\ln(A\beta42) = 0.724 \times \ln(A\beta38) + 0.251$, $R = 0.723$], but barely in MCI/AD ($R = 0.500$ for MCI; 0.393 for AD), and the MCI/AD plots were situated below the regression line for controls ($p < 0.001$, ANOVA). For a given Aβ42 value, the plot provided a higher Aβ38 measure in MCI/AD compared with controls.

These lower concentrations of Aβ42 appeared to be compensated with higher concentrations of Aβ38 as the levels of $\ln(A\beta38 + A\beta42)$ did not vary even in MCI/AD ($p = 0.293$, ANOVA). Thus, this points to the possibility that more Aβ42 and Aβ43 are converted to Aβ38 and Aβ40, respectively, in MCI/AD brains. According to numerical simulation based on the stepwise processing model, as the levels of βCTF decline to null, the levels of Aβ43 and 42 decrease and the ratios of Aβ40/43 and Aβ38/42 increase (unpublished observation). However, this situation can be excluded as the mechanism for lower concentrations of Aβ42 and 43, because the levels of βCTF have never been reported to be reduced in AD brains nor in plaque-forming Tg2576 mice that show lower CSF Aβ42 concentrations (Kawarabayashi et al, 2001). Thus, it is reasonable to suspect that the final cleavage steps from Aβ43 mostly to 40 and from Aβ42 to 38 are significantly enhanced in parallel (increases in released tri- and tetrapeptides) in brains affected by MCI/AD compared with controls (Fig 1).

This relationship in γ-secretase cleavage becomes clearer by plotting the product/precursor ratio representing cleavage efficiency at the step from Aβ42 to 38 (Aβ38/42) against that representing the cleavage efficiency at the step from Aβ43 to 40 (Aβ40/43) (Fig 4). The 'apparent' cleavage efficiency of Aβ43 was approximately 40-fold larger than that of Aβ42. The two ratios in CSF samples from MCI/AD and control subjects were largely proportional to each other, indicating that the corresponding cleavage processes in the two lines are tightly coupled (Fig 4). All plots were situated on a distinct line [$\ln(A\beta38/42) = 0.748 \times \ln(A\beta40/43) - 2.244$, $R = 0.936$] and its close surroundings. An increase in the cleavage from Aβ43 to 40 (*i.e.* more Aβ43 is converted to Aβ40) accompanied an increase in the cleavage from Aβ42 to 38 and *vice versa*, although the mechanism underlying this coupling between the two product lines remains unknown. This reminds us of the 'NSAID effect' in the 3-([3-cholamidopropyl]dimetylammonio)-2-hydroxy-1-propanesulfonate (CHAPSO)-reconstituted γ-secretase system (Takami et al, 2009; Weggen et al, 2001) in which the addition of sulindac sulfide to the γ-secretase reaction mixture, as expected, significantly suppressed Aβ42 production and increased Aβ38 production presumably by increasing the amounts of released tetrapeptide (VVIA) (Takami et al, 2009) and other peptides.

Most importantly, this graph provides a clear distinction between the control and MCI/AD groups (Fig 4; Aβ40/43 for MCI/AD *vs.* control, $p = 0.000$; Aβ38/42 for MCI/AD *vs.* control, $p = 0.000$; ANOVA, followed by Dunnett's *t*-test). The control values plotted close to the origin, whereas those for MCI/AD patients were distant from the origin along the line [$\ln(A\beta38/42) = 0.748 \times \ln(A\beta40/43) - 2.244$, $R = 0.936$]. It is also of note

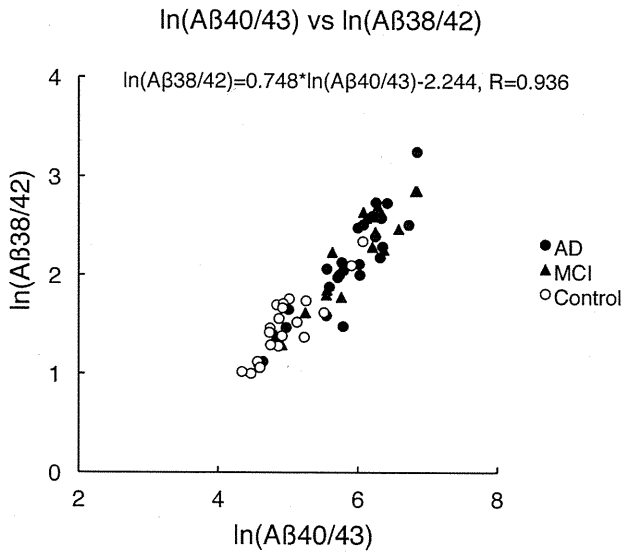

Figure 4. Ln(Aβ40/43) *versus* ln(Aβ38/42) plot. The ratios represent the cleavage efficiency at the final step of each line. Both ratios are largely proportional to each other ($y = 0.748 \times -2.244$, $R = 0.936$) and plots are located on the line and its close surroundings. This plot clearly distinguishes between control subjects and MCI/AD patients (Aβ40/43 for MCI *vs.* control, $p = 0.000$; Aβ38/42 for MCI *vs.* control, $p = 0.000$; ANOVA, followed by Dunnett's *t*-test). Control plots [open circles ($n = 21$)] are located close to the origin and MCI/AD plots [closed triangles ($n = 19$) and closed circles ($n = 24$), respectively] are a little distant from the origin.

that there was no significant difference between MCI and AD patients (Fig 4; Aβ40/43 for AD *vs.* MCI, $p = 1.000$; Aβ38/42 for AD *vs.* MCI, $p = 1.000$; Bonferroni's *t*-test). Two control values were a little farther from the origin, which may suggest that these subjects already have latent Aβ deposition or are in the preclinical AD stage. Additionally, we examined quite a small number of CSF samples from presenilin (PS) 1-mutated (symptomatic) familial AD (FAD) patients (T116N, L173F, G209R, L286V and L381V). Out of the three FAD cases near the regression line, two (T116N and L286V) were distant from the origin like sporadic AD cases and one (L381V) was closer to the origin than controls (both Aβ42/43 levels were lower than control; unpublished data). The remaining two (G209R and L173F) were extremely displaced from the line. Thus, a larger number of FAD cases are needed to give an appropriate explanation for their unusual characteristics in the plot, and the alteration of CSF Aβs shown above seems to be applicable only for sporadic AD.

Altogether, in MCI/AD, more Aβ42 and 43 are processed to Aβ38 and 40, respectively, than in controls. Even in MCI/AD, strict relationships are maintained between the levels of Aβ42 and Aβ43, and between those of Aβ38 and Aβ40 as seen in controls, which are predicted by the stepwise processing kinetics (unpublished observation). Thus, our observations suggest that lower CSF concentrations of Aβ42 and 43 and presumably higher CSF concentrations of Aβ38 and 40 are the consequence of altered γ-secretase activity in brain rather than the effect of preferential deposition of the two longer Aβ species (Aβ42 and 43) in senile plaques, which would not have maintained such strict relationships between the four Aβ species in CSF.

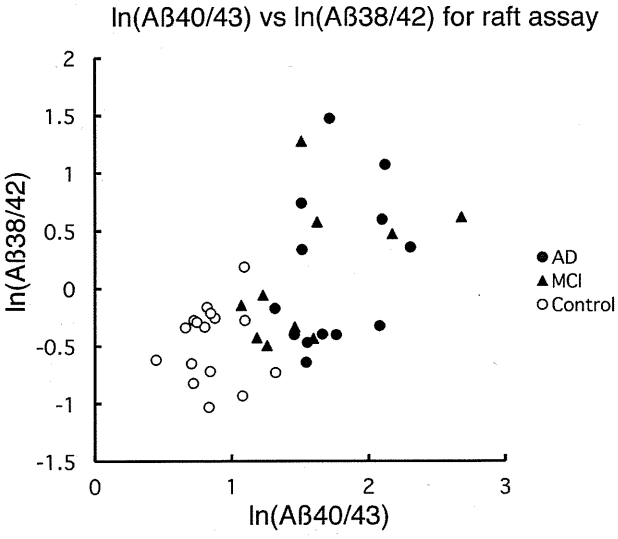

Figure 5. Ln(Aβ40/43) *versus* ln(Aβ38/42) plot based on direct quantification of raft-associated γ-secretase activity. The raft-associated γ-secretase prepared from control and MCI/AD brain specimens was incubated with βCTF for 2 h at 37°C (see Materials and Methods Section). Produced Aβs were quantified by Western blotting using specific antibodies. This plot distinguishes between control subjects and MCI/AD patients (Aβ40/43 for control *vs.* MCI/AD, $p < 0.001$; Aβ38/42 for control *vs.* MCI/AD, $p = 0.001$; Welch's *t*-test). MCI/AD plots [closed triangles ($n = 10$) and closed circles ($n = 13$), respectively] are as a whole a little distant from the origin, whereas control plots [open circles ($n = 16$)] are close to the origin.

To further test our hypothesis, we directly measured γ-secretase activities associated with lipid rafts isolated from AD, MCI and control cortices (Brodmann areas 9–11). For definite confirmation of the Aβ species, the reaction mixtures were subjected to quantitative Western blotting using specific antibodies rather than ELISA. At time 0, deposited Aβ42/43 species were detected in rafts from MCI/AD brains but not in control specimen (Supporting Information Fig S3). The amounts of ln(Aβ38 + Aβ42), which reflect the total capacity of the Aβ38/42-producing line, did not vary between AD, MCI and controls (Supporting Information Fig S4; $p = 0.969$, ANOVA). Thus, the gross activities of raft γ-secretase were comparable among the three groups. However, the plotted values for Aβ40/43 *versus* Aβ38/42 are divided into two groups: MCI/AD and controls (Fig 5; Aβ40/43 for control *vs.* MCI/AD, $p < 0.001$; Aβ38/42 for control *vs.* MCI/AD, $p = 0.001$; Welch's *t*-test) in the same way as those derived from CSF (Fig 4). It is notable that Figs. 4 and 5 are based on different methods, ELISA and Western blotting, respectively, but give similar results. There were no significant differences between MCI and AD specimen, although MCI patients (91 ± 4.9-year-old) were older than controls (77 ± 6.5-year-old) or AD patients (80 ± 5.0-year-old) (Aβ40/43 for MCI *vs.* AD, $p = 0.342$; Aβ38/42 for MCI *vs.* AD, $p = 0.911$). There were similar significant differences between control *versus* AD in the groups of which the ages were not significantly different (Aβ40/43 for control *vs.* AD, $p < 0.001$; Aβ38/42 for control *vs.* AD, $p = 0.03$).

DISCUSSION

Here, we assume that (i) Aβs in CSF are produced exclusively by γ-secretase in the brain, possibly in neurons; and (ii) Aβs in CSF are in the steady state. With these assumptions, the combined measurement of four Aβ species in CSF should predict the activity of γ-secretase in the brain. Here, the alterations in the γ-secretase activities do not mean the gross activity, *i.e.* total Aβ production, but the cleavage efficiency of the intermediates, Aβ42 and Aβ43.

In the present study, we quantified in CSF the four Aβ species, Aβ38/42 and Aβ40/43, but the Western blotting indicated the presence of additional Aβ species, Aβ37 and 39, in CSF (Supporting Information Fig S2). At present, we cannot exclude the possibility that a certain carboxyl terminus-specific protease(s) in CSF acts on the pre-existing Aβ species and converts them to Aβ37 and 39 (Zou et al, 2007). However, according to our unpublished data (Takami et al, unpublished observations), it is plausible that Aβ37 is derived from Aβ40, whereas Aβ39 is derived from Aβ42. Even if so, these pathways are very minor (~20–100-fold less) compared to the two major pathways, Aβ42 to Aβ38, and Aβ43 to Aβ40, when assessed by a reconstituted system (Takami et al, 2009). Thus, such strict relationships between four Aβs may have been relatively independent of Aβ37 and 39. The detailed relationship between all Aβs in the CSF awaits further quantification of the additional two Aβ species.

Currently, we do not know why the observation that Aβ40 is higher in MCI/AD CSF has so far not been reported except a recent paper (Simonsen et al, 2007). In fact, some of us previously reported no significant differences in CSF Aβ40 between AD and control subjects using a different ELISA (Shoji et al, 1998). It may be notable that we used newly constructed ELISA for Aβ40 based on a different set of monoclonal antibodies and thus, those discrepancies may come from the different antibody/epitope combination used for ELISA and/or different assay methods. In particular, it should be noted that all ELISAs used here detect Aβ1-x only, but not amino-terminally truncated forms. In this context, the ratio of Aβ40/43 appears to be more informative to discriminate between control and MCI/AD than the absolute levels of Aβ40 alone (Table 1 and Fig 5). It is possible that even if Aβ40 is not different between control and MCI/AD, the ratio Aβ40/43 could discriminate them.

We are the first to measure CSF Aβ43 using ELISA. The CSF concentrations of Aβ43 are 10-fold less than those of Aβ42. Nevertheless, the specificity of the newly constructed ELISA made the quantification of accurate levels of Aβ43 possible (Supporting Information Fig S1). Regarding the Aβ43 measures, we observed that its behaviour is entirely similar to that of Aβ42 in MCI/AD. Our preliminary observations using immunocytochemistry and ELISA quantification strongly suggest that Aβ43 deposits in aged human brains at the same time as Aβ42 (unpublished observations). Furthermore, Saido and colleagues have only recently reported that a PS1 R278I mutation in mice (heterozygous) caused an elevation of Aβ43 and its early and pronounced accumulation in the brain (Saito et al, 2011). It is possible that the cleavage of βCTF by this R278I γ-secretase may

be profoundly suppressed in the third cleavage step of the product line 1 (see Fig 1), which would result in negligible levels of Aβ40 and unusually high levels of Aβ43 (Nakaya et al, 2005). These results suggest that the role of Aβ43 should be reconsidered for the initiation of β-amyloid deposition and thus in AD pathogenesis.

Lower CSF concentrations of Aβ42 and 43 are not exclusively limited to MCI/AD. For example, similar low concentrations of Aβ42 and 43 were found in the CSF from eight patients with idiopathic normal pressure hydrocephalus (iNPH) (Aβ42, 76.3 ± 37.3 pM, $p = 0.012$ compared to controls: Aβ43, 5.2 ± 2.9 pM, $n = 8$, $p = 0.004$ compared to controls: Bonferroni's *t*-test; Silverberg et al, 2003). Thus, lower CSF concentrations of Aβ42 and 43 alone were unable to distinguish between iNPH and MCI/AD, and further, it is claimed that the former is often associated with abundant senile plaques, raising the possibility that Aβ deposition is enhanced by iNPH (Silverberg et al, 2003). However, when their partners Aβ38 and 40 were measured in CSF, both were found not to be significantly increased in iNPH (Aβ38, 459.2 ± 138.5 pM, $p = 0.484$ compared to controls; Aβ40, 1094.4 ± 375.3 pM, $n = 8$, $p = 0.103$ compared to controls; Table 1) in sharp contrast to MCI/AD indicating that the cleavage in iNPH at the steps from Aβ43 to 40 and from Aβ42 to 38 is not enhanced as it is in MCI/AD. Thus, it may be that the dilution effect elicited by ventricular enlargement would be the cause of lower CSF Aβ42 and 43 found in iNPH.

Currently, we do not know the mechanism behind the altered activity of brain γ-secretase in MCI/AD (Fig 4). First, it is of note that rafts prepared from MCI/AD brains but never from control brains at SP stage 0/A accumulated Aβ42 and Aβ43 (Supporting Information Fig S3; Oshima et al, 2001). It is possible that raft-deposited Aβ42/43 could induce a change in the γ-secretase activity, although the extent of the alteration in the activity appears not to be related to the extent of accumulation (unpublished observation). In this regard, it is of interest to note that Tg2576 mice, the best characterized AD animal model, shows reduced levels of Aβ42 in plasma as well as in CSF at the initial stage of Aβ deposition (Kawarabayashi et al, 2001). If the assumption here is correct, this may suggest that γ-secretase that produces plasma Aβs could also be altered. However, thus far, we have failed to replicate significantly lower Aβ42 levels or Aβ42/Aβ40 ratios in plasma from AD patients.

Second, there could be heterogenous populations of γ-secretase complexes that have distinct activities due to subtle differences in their components. γ-Secretase is a complex of four membrane proteins including PS, nicastrin (NCT), anterior pharynx defective 1 (Aph1) and presenilin enhancer 2 (Pen 2) (Takasugi et al, 2003). Aph 1 has three isoforms, and each can assemble active γ-secretase together with other components (Serneels et al, 2009). NCT, a glycoprotein, is present in immature and mature forms (Yang et al, 2002). The abundance of these heterogenous populations of proteins in the brain is probably under strict control. During MCI/AD, a certain population could replace other populations of γ-secretase and thus may show a distinct activity as a whole.

The data shown here represent only a cross-sectional study, but our keen interest is how the CSF levels of the four Aβ species would shift during the longitudinal course in an individual who is going to develop sporadic AD. Does one have any period during life when Aβ42 and 43 are at higher levels in CSF, and thus the ratios of Aβ38/42 and Aβ40/43 are smaller? At this period when the final cleavage steps of γ-secretase would be suppressed, the ISF concentrations of Aβ43 and 42 would increase, which would start or promote their aggregation in the brain parenchyma. If so, during life span, the individual's plot would move down along the regression line and move up as senile plaques accumulate, and the individual would eventually develop sporadic AD. However, thus far the period when there are increases in CSF Aβ42/43 has never been reported for sporadic AD. Nor has it been reported for asymptomatic FAD carriers (Ringman et al, 2008), whereas their plasma is known to contain higher levels (and percent) of Aβ42 (Kosaka et al, 1997; Ringman et al, 2008; Scheuner et al, 1996). It is likely that the stage of normal cognition and Aβ accumulation already accompanies reduced CSF Aβ42. If so, the alterations of γ-secretase should continue on for decades. Most interestingly, this alteration of CSF Aβ regulation seems to be planned to prevent further accumulation of Aβ42 and 43 in the brain.

However, Hong et al (2011) have recently shown, using *in vivo* microdialysis to measure ISF Aβ in APP transgenic mice, that the increasing parenchymal Aβ is closely correlated with decreasing ISF Aβ, suggesting that produced Aβ42 is preferentially incorporated into existing plaque-Aβ. This is a prevailing way of the interpretation of the data. Another way of the interpretation of data would be that during aging from 3 to 24 months, γ-secretase activity becomes altered and produces decreasing amounts of Aβ but with an increasing ratio of Aβ38/42 (and Aβ40/43). It is worth to mention that produced Aβ42 (but not Aβ40) appears to be selectively bound to rafts (from CHO cells) after long incubation (>4 h; Wada et al, unpublished observation). Also of note is that we quantified the total (free and bound) Aβ produced by an *in vitro* reconstituted system (Fig 5). What is claimed here is that decreased levels of CSF Aβ42 are largely due to alterations of γ-secretase activity rather than due to selective deposition of Aβ42 in preexisting plaques. What proportions of decreased ISF (CSF) Aβ42 levels would be contributed to by altered γ-secretase activity and selective deposition of Aβ42/43 to parenchymal plaques awaits future studies.

Finally, our observation has therapeutic implication. As shown elsewhere and here above, if Aβ42 is the culprit for MCI/AD, non-steroidal anti-inflammatory drugs (NSAIDs) would have been quite a reasonable therapeutic compound, which enhances cleavage at the third step in the stepwise processing, leading to lower levels of Aβ42 without greatly interfering with the Aβ bulk flow (Weggen et al, 2001). This sharply contrasts with some of the γ-secretase inhibitors currently under development and in clinical trial, which block the Aβ bulk flow. However, the present study raises the possibility that even if NSAIDs are administered, the expected beneficial effect could be minimal in MCI/AD patients, because in these patient brains, γ-secretase is already shifted to an NSAID-like effect.

MATERIALS AND METHODS

Subjects

Cerebrospinal fluid samples from 24 AD patients (mild to moderate AD; 50–86 years old), 19 MCI patients (57–82 years old) and 21 control subjects (61–89 years old) were collected (see Table 1) at Department of Neurology, Hirosaki University Hospital and at Department of Geriatrics and Gerontology, Tohoku University Hospital, and at Department of Neurology, Niigata University Hospital. The CSF samples from (symptomatic) 5 FAD (mPS1) patients (T116N, L173F, G209R, L286V and L381V) were from Niigata University Hospital. Probable AD cases met the criteria of the National Institute of Neurological and Communicative Disorders and Stroke–Alzheimer's Disease and Related Disorders (NINCDS-ADRDA) (Kuwano et al, 2006; McKhann et al, 1984). Additional diagnostic procedures included magnetic resonance imaging. Dementia severity was evaluated by the Mini-Mental State Examination (MMSE). Diagnosis of MCI was made according to the published criteria (Winblad et al, 2004). Diagnosis of iNPH was made according to the guideline issued by the Japanese Society of NPH (Ishikawa et al, 2008). Controls who had no sign of dementia and lived in an unassisted manner in the local community were recruited. All individuals included in this study were Japanese and 24 AD patients examined here were judged to have sporadic AD because of negative family history. This study was approved by the ethics committee at each hospital or institute.

Human cortical specimens for quantification of raft-associated γ-secretase activity were obtained from those brains that were removed, processed and placed in −80°C within 12 h postmortem [Patients were placed in a cold (4°C) room within 2 h after death] at the Brain Bank at Tokyo Metropolitan Institute of Gerontology. For all the brains registered at the bank we obtained written informed consents for their use for medical research from patient or patient's family. Each brain specimen (~0.5 g) were taken from Brodmann areas 9–11 of 13 AD patients [80 ± 5.0 years of age, Braak NFT stage > IV, SP stage = C (retrospective) CDR ≫ 1], 10 MCI patients (91 ± 4.9 years of age, Braak NFT stage < IV, SP stage < C, CDR = 0.5) and 16 controls (77 ± 6.5 years of age, Braak NFT stage < I, SP stage = 0/A, CDR = 0) (Adachi et al, 2010; Li et al, 1997).

Cerebrospinal fluid analysis

Cerebrospinal fluid (10–15 ml) was collected in a polypropylene or polystyrene tube and gently inverted. After brief centrifugation CSF was aliquotized to polypropylene tubes (0.25–0.5 ml), which were kept at −80°C until use. In our experience, Aβ42 (possibly, other Aβ species too) are readily absorbed even to polypropylene tubes (~20% per new exposure, as shown by Luminex xMAP quantification), and repeated aliquotization to new tubes may cause profoundly lower measures of Aβs (Tsukie and Kuwano, unpublished data, 2010). This may partly explain why absolute levels of Aβs in CSF greatly vary among laboratories, whereas their relative ratios (*e.g.* Aβ42/40) seem to be roughly consistent. The CSF concentrations of Aβ38, 40 and 42 were quantified using commercially available ELISA kits (Cat no. 27717, 27718 and 27712, respectively, IBL, Gunma, Japan). To measure Aβ43, anti-Aβ43 polyclonal antibody as a capture antibody was combined with amino terminus-specific antibody (82E1) (Cat no. 10323, IBL, Gunma, Japan) as a detector antibody. The detection limit of Aβ43 quantified by the ELISA was 0.78 pM (data not shown). Thus all ELISAs used here detect Aβ1-x, but not amino-terminally truncated Aβs. The specificities of ELISAs are provided in Supporting Information Fig S1.

CSF immunoprecipitation and Western blotting

When required, CSF Aβs were immunoprecipitated with protein G-sepharose conjugated with 82E1 at 4°C by keeping a container in gentle rotation overnight. The mixture was centrifuged at 10,000×g for 5 min, and resultant pellets were then washed twice with phosphate-buffered saline. The washed beads were suspended with the Laemmli sample buffer for SDS–polyacrylamide gel electrophoresis (SDS–PAGE). The immunoprecipitated Aβs were separated on Tris/Tricine/8 M urea gels (Kakuda et al, 2006), followed by Western blotting using 82E1. To immunodetect Aβ42 and Aβ43, Aβ42 monoclonal antibody (44A3, IBL) and Aβ43 polyclonal antibody (IBL) were used (Supporting Information Fig S3).

Numerical simulation based on the stepwise processing model of γ-secretase

The temporal profiles for the ratios of Aβ40/43 and Aβ38/42 were simulated based on the stepwise processing model. Parameters including rate constants were set to fit maximally the temporal profile of the cleaving activity in the reconstituted γ-secretase system (Takami et al, 2009).

We set the condition that βCTF substrate is supplied steadily from the external source. When βCTF supply is balanced roughly in the order with γ-secretase processing rate, the stepwise-processing model was found to have the two successive steady states, with each accompanying linear changes in [ES] or [S] concentrations. The first steady state is just after the initial transition period that corresponds to the acute saturation phase of γ-secretase with βCTF. The second steady state is associated with the constant concentrations of the enzyme/substrate complex except ES38 and ES40. Because these steady states kept the ratios of Aβ38/Aβ40 and Aβ42/Aβ43 constant, the simulation was quite consistent with the CSF data.

Quantification of human brain raft-associated γ-secretase activity

Since γ-secretase is thought to be concentrated in rafts (Hur et al, 2008; Wada et al, 2003), we measured raft-associated γ-secretase activity rather than CHAPSO-solubilized activity. Rafts were prepared from human brains which were frozen within 12 h postmortem, as previously described (Oshima et al, 2001; Wada et al, 2003) with some modifications. We do not know exactly whether the γ-secretase activity depends upon the sampling site. In our hands, there appear no large differences in the activity among the sampled sites in a given prefrontal slice. No significant differences in the activity were noted between outer and inner layer of the cortex. After carefully removing leptomeninges and blood vessels, small (<0.5 g) blocks from prefrontal cortices (Brodmann areas 9–11) were homogenized in ~10 volumes of 10% sucrose in MES-buffered saline (25 mM MES, pH 6.5, and 150 mM NaCl) containing 1% CHAPSO and various protease inhibitors. The homogenate was adjusted to 40% sucrose by the addition of an equal volume of 70% sucrose in MES-buffered saline, placed at the bottom of an ultracentrifuge tube, and overlaid with 4 ml of 35% sucrose and finally with 4 ml of 5% sucrose in MES-buffered saline. The discontinuous gradient was centrifuged at 39,000 rpm for 20 h at 4°C on a SW 41 Ti rotor (Beckman, Palo

The paper explained

PROBLEM:

Alzheimer's disease is a devastating form of progressive dementia, in which senile plaques composed of Aβ form in the brain. Different species of Aβ are derived from APP through sequential cleavage by β- and γ-secretases and can be detected in the CSF of patients. These can serve as markers for the disease.

RESULTS:

We investigated why CSF concentrations of Aβ42 are lower in MCI and AD patients. We suggest that this is not because Aβ42/43 is selectively deposited in the brain, but because γ-secretase activity is altered in AD brain: more Aβ42 and Aβ43 are converted to Aβ40 and Aβ38, respectively, resulting in lower Aβ42 and Aβ43 in CSF.

IMPACT:

Our results predict that γ-secretase modulators would have only limited efficacy in treatment of AD patients, because Aβ42/43 production by γ-secretase is already shifted towards reduced levels in AD brain.

Alto, CA). An interface of 5%/35% sucrose (fraction 2) was carefully collected (referred to as raft fraction). Raft fractions were recentrifuged after dilution with buffer C (20 mM PIPES, pH 7.0, 250 mM sucrose and 1 mM EGTA). The resultant pellet was washed twice and resuspended with buffer C, which was kept at −80°C until use.

As the method of measuring the raft γ-secretase activity was not yet established, we first determined the assay conditions. The incubation of raft fraction with βCTF generated exactly the same tri- and tetrapeptides we previously observed in the detergent-soluble γ-secretase assay system (Takami et al, unpublished observation). This suggests that the cleavage by raft-associated γ-secretase proceeds in the identical manner as by CHAPSO-reconstituted γ-secretase (Takami et al, 2009). In our hands, preexisting βCTF bound in rafts generated only negligible amounts of Aβs, and their generation was dependent exclusively on exogenously added βCTF. Thus, we concluded that the addition of βCTF to raft fraction make possible to measure the raft-associated γ-secretase activity, although we do not know how the exogenously added βCTF is integrated into raft, gets access to and is degraded by raft-embedded γ-secretase. Using this assay method, the activities of raft-associated γ-secretase in human brains were found to be only a little affected postmortem, when compared with that prepared from fresh rat brains. A progressive decline in the activity was barely detectable from 4 to 17 h postmortem. The discrepancy in the postmortem decay between our and the previous data (Hur et al, 2008) would be ascribed to the assay method: the latter are based on the activity measured by using endogenous (raft-bound) substrate that is also susceptible to proteolytic degradation (Hur et al, 2008).

Each raft fraction, adjusted to 100 μg/ml in protein concentration, was incubated with 200 nM C99FLAG for 2 h at 37°C (Kakuda et al, 2006). The produced Aβs were separated on SDS–PAGE, and subjected to quantitative Western blotting, using specific antibodies, 3B1 for Aβ38, BA27 for Aβ40, 44A3 for Aβ42 and anti-Aβ43 polyclonal for Aβ43.

Statistical analysis

All statistical analyses were performed using SPSS version 14.0. The results were expressed as means ± standard deviations. Because data transformations were required to achieve normally distributed data, all analyses including Aβ38, Aβ40, Aβ42 and Aβ43 were performed after a logarithmic transformation. Pearson's correlation coefficients were calculated to indicate the strength of the linear relationship between two variables. An ANOVA was used to test the equality of mean values of continuous variables among three groups, that is control, MCI and AD. Multiple comparisons were done by Dunnett's *t*-test, Bonferroni's *t*-test and Welch's *t*-test between control and MCI/AD, and among three groups, respectively. A two-tailed *p*-value of <0.05 was considered to be statistically significant.

Author contributions

NK, MT, KN, YI: measurement of raft-associated γ-secretase activity in human brains, LC-MS/MS confirmation of released peptides, ELISA quantification of Aβ38, 40, 42 and 43 in CSF and tissue blocks, and experimental design of the present work; MS, HiA, KF, TI, and the Japanese Alzheimer's Disease Neuroimaging Initiative: collection of CSF samples from controls, MCI/AD patients; YH, MM, HaA: collection of CSF from iNPH patients; HY, SM, HH: Aβ immunocytochemistry of tissue sections from brains with various SP stages (Braak); KA: statistical analysis; RK: establishment of the appropriate Aβ quantification conditions; YN: simulation of the stepwise processing model.

Acknowledgements

We thank Dr. Haruhiko Akiyama, Department of Psychogeriatrics, Tokyo Institute of Psychiatry, Tokyo Metropolitan Organization for Medical Research, Tokyo, for the help in the initial phase of this study, and Dr. Takaomi C. Saido, RIKEN Brain Science Institute, for sharing the data on his R278I transgenic mice. Dr. Makoto Higuchi, Molecular Imaging Center, National Institute of Radiological Sciences, Chiba, kindly provided us with aged Tg2576 littermates. This project was supported by New Energy and Industrial Technology Development Organization in Japan (J-ADNI).

Supporting Information is available at EMBO Molecular Medicine online.

The authors declare that they have no conflict of interest.

References

Adachi T, Saito Y, Hatsuta H, Funabe S, Tokumaru AM, Ishii K, Arai T, Sawabe M, Kanemaru K, Miyashita A, *et al* (2010) Neuropathological asymmetry in argyrophilic grain disease. J Neuropathol Exp Neurol 69: 737-744

Hong S, Quintero-Monzon O, Ostaszewski BL, Podlisny DR, Cavanaugh WT, Yang T, Holtzman DM, Cirrito JR, Selkoe DJ (2011) Dynamic analysis of amyloid β-protein in behaving mice reveals opposing changes in ISF versus parenchymal Aβ during age-related plaque formation. J Neurosci 31: 15861-15869

Hur JY, Welander H, Behbahani H, Aoki M, Frånberg J, Winblad B, Frykman S, Tjernberg LO (2008) Active gamma-secretase is localized to detergent-resistant membranes in human brain. FEBS J 275: 1174-1187

Ishikawa M, Hashimoto M, Kuwana N, Mori E, Miyake H, Wachi A, Takeuchi T, Kazui H, Koyama H (2008) Guidelines for management of idiopathic normal pressure hydrocephalus. Neurol Med Chir (Tokyo) 48: S1-S23

Iwatsubo T, Odaka A, Suzuki N, Mizusawa H, Nukina N, Ihara Y (1994) Visualization of Aβ42(43) and Aβ40 in senile plaque with end-specific Aβ monoclonals: evidence that an initially deposited forms is Aβ42(43). Neuron 13: 45-53

Kakuda N, Funamoto S, Yagishita S, Takami M, Osawa S, Dohmae N, Ihara Y (2006) Equimolar production of amyloid β-protein and amyloid precursor protein intracellular domain from β-carboxyl-terminal fragment by γ-secretase. J Biol Chem 281: 14776-14786

Kawarabayashi T, Younkin LH, Saido TC, Shoji M, Ashe KH, Younkin SG (2001) Age-dependent changes in brain, CSF, and plasma amyloid (β) protein in the Tg2576 transgenic mouse model of Alzheimer's disease. J Neurosci 21: 372-381

Kosaka T, Imagawa M, Seki K, Arai H, Sasaki H, Tsuji S, Asami-Odaka A, Fukushima T, Imai K, Iwatsubo T (1997) The βAPP717 Alzheimer mutation increases the percentage of plasma amyloid-beta protein ending at Aβ42(43). Neurology 48: 741-745

Kuwano R, Miyashita A, Arai H, Asada T, Imagawa M, Shoji M, Higuchi S, Urakami K, Kakita A, Takahashi H, *et al* (2006) Dynamin-binding protein gene on chromosome 10q is associated with late-onset Alzheimer's disease. Hum Mol Genet 15: 2170-2182

Li G, Aryan M, Silverman JM, Haroutunian V, Perl DP, Birstein S, Lantz M, Marin DB, Mohs RC, Davis KL (1997) The validity of the family history method for identifying Alzheimer disease. Arch Neurol 54: 634-640

McKhann G, Drachman D, Folstein M, Katzman R, Price D, Stadlan EM (1984) Clinical diagnosis of Alzheimer's disease: report of the NINCDS-ADRDA Work Group under the auspices of Department of Health and Human Services Task Force on Alzheimer's Disease. Neurology 34: 939-944

Nakaya Y, Yamane T, Shiraishi H, Wang HQ, Matsubara E, Sato T, Dolios G, Wang R, De Strooper B, Shoji M, *et al* (2005) Random mutagenesis of presenilin-1 identifies novel mutants exclusively generating long amyloid β-peptides. J Biol Chem 280: 19070-19077

Oshima N, Morishima-Kawashima M, Yamaguchi H, Yoshimura M, Sugihara S, Khan K, Games D, Schenk D, Ihara Y (2001) Accumulation of amyloid beta-protein in the low-density membrane domain accurately reflects the extent of beta-amyloid deposition in the brain. Am J Pathol 158: 2209-2218

Qi-Takahara Y, Morishima-Kawashima M, Tanimura Y, Dolios G, Hirotani N, Horikoshi Y, Kametani F, Maeda M, Saiso TC, Wang R, *et al* (2005) Longer forms of amyloid β protein: implications for the mechanism of intramembrane cleavage by γ-secretase. J Neurosci 25: 436-445

Ringman JM, Younkin SG, Pratico D, Seltzer W, Cole GM, Geschwind DH, Rodriguez-Agudelo Y, Schaffer B, Fein J, Sokolow S, *et al* (2008) Biochemical markers in persons with preclinical familial Alzheimer disease. Neurology 71: 85-92

Saito T, Suemoto T, Brouwers N, Sleegers K, Funamoto S, Mihira N, Matsuba Y, Yamada K, Nilsson P, Takano J, *et al* (2011) Potent amyloidogenicity and pathogenicity of Aβ43. Nat Neurosci 14: 1023-1032

Scheuner D, Eckman C, Jensen M, Song X, Citron M, Suzuki N, Bird TD, Hardy J, Hutton M, Kukull W, *et al* (1996) Secreted amyloid β-protein similar to that in the senile plaques of Alzheimer's disease in increase in vivo by the presenilin 1 and 2 and APP mutations linked to familial Alzheimer's disease. Nat Med 2: 864-870

Schoonenboom NS, Mulder C, Van Kamp GJ, Mehta SP, Scheltens P, Blankenstein MA, Mehta PD (2005) Amyloid β 38, 40, and 42 species in cerebrospinal fluid: more of the same. Ann Neurol 58: 139-142

Selkoe DJ (2001) Alzheimer's disease: genes, proteins, and therapy. Physiol Rev 81: 741-766

Serneels L, Van Biervliet J, Craessaerts K, Dejaegere T, Horre K, Van Houtvin T, Esselmann H, Paul S, Schafer MK, Berezovska O, *et al* (2009) γ-Secretase heterogeneity in the Aph1 subunit: relevance for Alzheimer's disease. Science 324: 639-642

Shoji M, Matsubara E, Kanai M, Watanabe M, Nakamura T, Tomidokoro Y, Shizuka M, Wakabayashi K, Igeta Y, Ikeda Y, *et al* (1998) Combination assay of CSF tau, Aβ1–40 and Aβ 1–42(43) as a biochemical marker of Alzheimer's disease. J Neurol Sci 158: 134-140

Silverberg GD, Mayo M, Saul T, Rubenstein E, McGuire D (2003) Alzheimer's disease, normal-pressure hydrocephalus, and senescent changes in CSF circulatory physiology: a hypothesis. Lancet Neurol 2: 506-511

Simonsen AH, Hansson SF, Ruetschi U, McGuire J, Podust VN, Davies HA, Mehta P, Waldemar G, Zetterberg H, Andreasen N, *et al* (2007) Amyloid β1–40 quantification in CSF: comparison between chromatographic and immunochemical methods. Dement Geriatr Cogn Disord 23: 246-250

Takami M, Nagashima Y, Sano Y, Ishihara S, Morishima-Kawashima M, Funamoto S, Ihara Y (2009) γ-Secretase: successive tripeptide and tetrapeptide release from the transmembrane domain of β-carboxyl terminal fragment. J Neurosci 29: 13042-13052

Takasugi N, Tomita T, Hayashi I, Tsuruoka M, Niimura M, Takahashi Y, Thinakaran G, Iwatsubo T (2003) The role of presenilin cofactors in the γ-secretase complex. Nature 422: 438-441

Wada S, Morishima-Kawashima M, Qi Y, Misonou H, Shimada Y, Ohno-Iwashita Y, Ihara Y (2003) Gamma-secretase activity is present in rafts but is not cholesterol-dependent. Biochemistry 47: 13977-13986

Weggen S, Eriksen JL, Das P, Sagi SA, Wang R, Pietrzik CU, Findlay KA, Smith TE, Murphy MP, Bulter T, *et al* (2001) A subset of NSAIDs lower amyloidogenic Aβ42 independently of cyclooxygenase activity. Nature 414: 212-216

Winblad B, Palmer K, Kivipelto M, Jelic V, Fratiglioni L, Wahlund LO, Nordberg A, Backman L, Albert M, Almkvist O, *et al* (2004) Mild cognitive impairment—beyond controversies, towards a consensus: report of the International Working Group on Mild Cognitive Impairment. J Intern Med 256: 240-246

Yang DS, Tandon A, Chen F, Yu G, Yu H, Arakawa S, Hasegawa H, Duthie M, Schmidt SD, Ramabhadran TV, *et al* (2002) Mature glycosylation and trafficking of nicastrin modulate its binding to presenilins. J Biol Chem 277: 28135-28142

Zou K, Yamaguchi H, Akatsu H, Sakamoto T, Ko M, Mizoguchi K, Gong JS, Yu W, Yamamoto T, Kosaka K, *et al* (2007) Angiotensin-converting enzyme converts amyloid β-protein 1–42 (Aβ(1–42)) to Aβ(1–40), and its inhibition enhances brain Aβ deposition. J Neurosci 27: 8628-8635

Journal of Neuroscience Research

Journal of Neuroscience Research 89:815–821 (2011)

Dissociation of β-Amyloid From Lipoprotein in Cerebrospinal Fluid From Alzheimer's Disease Accelerates β-Amyloid-42 Assembly

Ayumi Takamura,[1,2] Takeshi Kawarabayashi,[2] Tatsuki Yokoseki,[3] Masao Shibata,[3] Maho Morishima-Kawashima,[4] Yuko Saito,[5] Shigeo Murayama,[5] Yasuo Ihara,[6] Koji Abe,[7] Mikio Shoji,[2] Makoto Michikawa,[1] and Etsuro Matsubara[1,2]*

[1]Department of Alzheimer's Disease Research, Research Institute, National Center for Geriatrics and Gerontology, Aichi, Japan
[2]Department of Neurology, Institute of Brain Science, Hirosaki University Graduate School of Medicine, Aomori, Japan
[3]Immunas Pharma Inc., Kanagawa, Japan
[4]Department of Molecular Neuropathology, Faculty of Pharmaceutical Sciences, Hokkaido University, Hokkaido, Japan
[5]Department of Neuropathology, Tokyo Metropolitan Institute of Gerontology, Tokyo, Japan
[6]Department of Neuropathology, Faculty of Life and Medical Sciences, Doshisha University, Kyoto, Japan
[7]Department of Neurology, Okayama University School of Medicine, Okayama, Japan

Monoclonal 2C3 specific to β-amyloid (Aβ) oligomers (AβOs) enabled us to test our hypothesis that the alteration of lipoprotein–Aβ interaction in the central nervous system (CNS) initiates and/or accelerates the cascade favoring Aβ assembly. Immunoprecipitation of frontal cortex employing 2C3 unequivocally detected soluble 4-, 8-, and 12-mers in Alzheimer's disease (AD) brains. Immunoblot analysis of the entorhinal cortex employing 2C3 revealed that the accumulation of soluble 12-mers precedes the appearance of neuronal loss or cognitive impairment and is enhanced as the Braak neurofibrially tangle (NFT) stages progress. The dissociation of soluble Aβ from lipoprotein particles occurs in cerebrospinal fluid (CSF), and the presence of lipoprotein-free oligomeric 2C3 conformers (4- to 35-mers) was evident, which mimic CNS environments. Such CNS environments may strongly affect conformation of soluble Aβ peptides, resulting in the conversion of soluble $Aβ_{42}$ monomers into soluble $Aβ_{42}$ assembly. The findings suggest that functionally declined lipoproteins may accelerate the generation of metabolic conditions leading to higher levels of soluble $Aβ_{42}$ assembly in the CNS.

Key words: Alzheimer's disease; Aβ; lipoprotein; oligomer; monomer

Accumulating lines of evidence indicate that memory loss represents a synaptic failure caused directly by soluble β-amyloid (Aβ) oligomers (AβOs; Klein et al., 2001; Selkoe, 2002; Hass and Selkoe, 2007). The possible mechanism underlying the neurotoxic action of AβOs has been postulated as neurotoxic ligands (Lambert et al., 1998; Walsh et al., 2002; Chromy et al., 2003; Gong et al., 2003; Lacor et al., 2004; Cleary et al., 2005; Lesné et al., 2006; Shankar et al., 2008; Noguchi et al., 2009), iron channel formation (Lin et al., 2001; Quist et al., 2005), pore formation (Lashuel et al., 2002; Kayed et al., 2009), and dysfunction of cholesterol metabolism in neurons (Michikawa et al., 2001; Gong et al., 2002; Zou et al., 2002). However, the exact metabolic conditions controlling the in vivo generation of soluble AβOs remain unknown. It is well known that aging is the most prevailing risk factor for sporadic AD. In vivo studies have shown that Aβ neurotoxicity is closely related to the brain aging via unknown age-related factors (Geula et al., 1998), perhaps reflecting metabolic alterations. Notably, the APOE genotype is also the major genetic risk factor for late-onset sporadic AD (Schmechel et al., 1993; Tanzi and Bertram, 2001; Wellington, 2004). HDL-like lipoproteins, mainly

Contract grant sponsor: Ministry of Education, Culture, Sports, Science and Technology, Japan (to E.M.); Contract grant sponsor: the Program for Promotion of Fundamental Studies in Health Sciences of the National Institute of Biomedical Innovation (NIBIO; to E.M.).

*Correspondence to: Etsuro Matsubara, Department of Neurology, Institute of Brain Science, Hirosaki University Graduate School of Medicine, 5 Zaifu, Hirosaki, Aomori 036-8216, Japan. E-mail: etsuro@cc.hirosaki-u.ac.jp

Received 7 September 2010; Revised 17 December 2010; Accepted 11 January 2011

Published online 10 March 2011 in Wiley Online Library (wileyonlinelibrary.com). DOI: 10.1002/jnr.22615

lipidated apoE, are in charge of cholesterol transport to and from neurons (Michikawa et al., 2001; Gong et al., 2002), in which cholesterol metabolism is quite different from that in systemic circulation. In addition to lipid trafficking, apoE as a form of HDL-like lipoprotein plays a major role in Aβ metabolism in the central nervous system (CNS). Under physiological conditions, HDL-like lipoproteins unequivocally interact with soluble Aβ in cerebrospinal fluid (CSF; Koudinov et al., 1996). Interestingly, when the generation of HDL-like lipoproteins in the AD mouse model is suppressed or overexpressed via the specific regulation of ATP-binding cassette A1 (ABCA1), Aβ deposition exhibits augmentation or reduction, respectively, which depends on the degree of ABCA1-mediated lipidation of apoE in the CNS (Wahrle et al., 2005, 2008). From these points of view, lipidic environments in the CNS represent one of the prevailing metabolic conditions. We hypothesized that an alteration of the lipoprotein–sAβ interaction in the CNS is capable of initiating and/or accelerating the cascade favoring Aβ assembly. Actually, we demonstrate that functionally declined lipoproteins may be the major determinants in the generation of metabolic conditions leading to higher levels of the soluble dimeric form of Aβ in AD brains (Matsubara et al., 1999, 2004). To verify this hypothesis and extend previous observations (Matsubara et al., 1999, 2004), we focused on the entorhinal cortex (EC) as well as CSF, which mimics CNS environments, followed by biochemical analyses using an antioligomer specific antibody. The presence of lipoprotein-free soluble AβOs in CSF was assessed in age-matched normal controls (NCs) and patients with Alzheimer's disease (AD) by size-exclusion chromatography (SEC) and enzyme-linked immunosorbent assay (ELISA) specific for either AβOs or AβMs to test our hypothsis.

MATERIALS AND METHODS

Generation of Monoclonal 2C3

Monoclonal 2C3, which is specific to AβOs with a molecular mass larger than tetramers (unpublished data), was generated and characterized as described elsewhere.

Patients

CSF samples (5 ml) were collected from 13 age-matched normal controls (NCs; 70.6 ± 8.2 years old) and 12 AD patients (73.2 ± 7.8 years old) after 12 hr of fasting. None of the individuals in the two groups had a history of stroke or other neurological conditions in the CNS that might have affected their lipoprotein profile, and none was taking drugs known to affect lipid metabolism. The diagnosis of AD was made in accordance with the NINCDS-ADRDA criteria, and only those who met the criteria of probable AD were included.

Lipoprotein Separation and Depletion

After separation of CSF collected from 12 patients with AD and 13 NCs, lipoprotein depletion was carried out by preparative sequential density flotation ultracentrifugation using 600 μl of CSF and a protocol previously described (Matsubara et al., 2004). Briefly, the density of the collected CSF was adjusted to 1.25 g/ml using KBr, and the CSF was ultracentrifuged at 100,000 rpm for 8 hr at 16°C using a Hitachi RP100AT rotor. The infranatant at a density of 1.25 g/ml, named lipoprotein-depleted CSF (LPD-CSF), and the floated lipoproteins were subjected to ultrafiltration using a 3-kDa cutoff membrane (Microcon 3; Amicon, Inc.) and stored either frozen or at 4°C until use.

SEC

SEC (molecular exclusion, 2×10^6; void volume varied from fraction (Fr.) 7 to Fr. 9 enabled us to separate specifically not only AβMs from AβOs, but also lipoprotein-associated Aβ from lipoprotein-free Aβ, as previously reported (Matsubara et al., 2004). The Aβ species either in whole CSF or in lipoprotein-depleted CSF were fractionated on a Superose 12 size-exclusion column (1 cm × 30 cm; Pharmacia, Uppsala, Sweden) equilibrated with the corresponding mobile-phase solution at a flow rate of 0.5 ml/min. Twenty-eight fractions of 1 ml each were collected and analyzed. Lipoprotein was depleted as described previously (Matsubara et al., 2004). Details are also described below. To determine where Aβ eluted, a 100-μl aliquot from each fraction was analyzed in a BNT77-BC05 or BNT77-BA27 enzyme-linked immunosorbent assay (ELISA) as described previously in detail (Matsubara et al., 2004). For evaluation of lipids, total cholesterol levels were enzymatically measured using a standard kit (Wako, Osaka, Japan). Under our experimental conditions, CSF lipoproteins were eluted in Frs. 7–14, whereas Frs. 15–28 contained cholesterol-free proteins. To determine further where the Aβ oligomers eluted, a 100-μl aliquot from each fraction was analyzed by 2C3-based oligomer sandwich ELISA.

Human Tissue Subjects and Extractions

The current study is based on autopsy cases (n = 50; 26 men, 24 women) from the Brain Bank at the Tokyo Metropolitan Institute of Gerontology (Itabashi, Tokyo, Japan). All of the subjects and the sampling methods were reported previously in detail (Katsuno et al., 2005). In this project, we focused on the soluble brain fraction, which was not characterized in a previous study (Katsuno et al., 2005). Briefly, frozen tissue samples (the anterior portion of the entorhinal cortex) were homogenized in 9 volumes of Tris-saline (TS) buffer containing a cocktail of protease inhibitors as described previously (Katsuno et al., 2005). The homogenates were centrifuged at 265,000*g* for 20 min. One-third (0.5 ml) of the homogenates was subjected to 2C3 immunoblot analysis.

ELISA Specific for Either AβMs or AβOs in CSF

After informed consent had been obtained, CSF samples were collected and stored in the human resource bank of the Department of Neurology, Okayama University School of Medicine. All human age-matched CSF samples were randomly selected from this bank and used for this study. To characterize the presence of AβOs in CSF, the CSF samples were subjected to SEC as described above. To determine

where Aβ was eluted, 100-μl fractions were analyzed by AβM-specific BNT77-BA27 or BNT77-BC05 ELISA as described previously in detail (Matsubara et al., 2004). With regard to ELISA specific for AβOs, a chemiluminescence-based ELISA was carried out to detect specifically AβOs, not monomeric Aβ. Microplates (Maxisorp White Microplate; Nunc, Roskilde, Denmark) were precoated with monoclonal 2C3 (IgG2b isotype) and sequentially incubated for 24 hr at 4°C with 100 μl of different samples, followed by 24-hr incubation at 4°C with horseradish-peroxidase-conjugated BA27 Fab′ fragment (anti-$A\beta_{1-40}$ antibody, specific for $A\beta_{40}$; Wako) or horseradish-peroxidase-conjugated BC05 Fab′ fragment (anti-$A\beta_{35-43}$ antibody, specific for $A\beta_{42}$, Wako). Chemiluminescence was developed using SuperSignal ELISA Pico Chemiluminescent substrate (Pierce, Rockford, IL) on a Veritas microplate luminometer (Promega, Madison, WI).

Human Materials Including Brain and CSF

All human brains were used under a protocol provided by the human studies committee for research-related use of human materials of the Faculty of Medicine, University of Tokyo; Tokyo Metropolitan Institute of Gerontology; Tokyo Metropolitan Geriatric Hospital; and National Center for Geriatrics and Gerontology. This research project was approved by the local ethical committee of the Faculty of Medicine, University of Tokyo; Tokyo Metropolitan Institute of Gerontology; Tokyo Metropolitan Geriatric Hospital; and National Center for Geriatrics and Gerontology.

Statistical Analyses

We used factorial design analysis of variance (ANOVA) or Student's unpaired *t*-test to analyze data as appropriate. Significant ANOVA values were subsequently subjected to analyses of simple main effects or post hoc comparisons of individual means using Tukey's or Dunnett's method as appropriate. We considered $P \leq 0.05$ as significant for all studies.

RESULTS AND DISCUSSION

We determined the ability of monoclonal 2C3 to capture Aβ oligomers in AD-affected brains. Multiple "saline-soluble" Aβ species with molecular masses corresponding to those of 1-, 2-, 4-, 8-, and 12-mers were immunoprecipitated using monoclonal 6E10 from the cerebral cortex of the AD brain (Fig. 1A, lane 1). In contrast, monoclonal 2C3 unequivocally retrieved "soluble" 4-, 8-, and 12-mers from the AD brain (Fig. 1A, lane 2), but not those from the control brain (Fig. 1A, lane 3) under the conditions studied. These findings clearly demonstrated that monoclonal 2C3 is specific to AβOs, not AβMs.

Among the soluble oligomers identified, 12-mer has been shown as a candidate Aβ assembly responsible for plaque-independent cognitive decline in AD (Lesné et al., 2006). We then assessed the levels of 12-mer in saline-soluble fractions by immunoblotting using monoclonal 2C3 in 50 autopsy cases as previously reported (Katsuno et al., 2005): the entorhinal cortices (ECs)

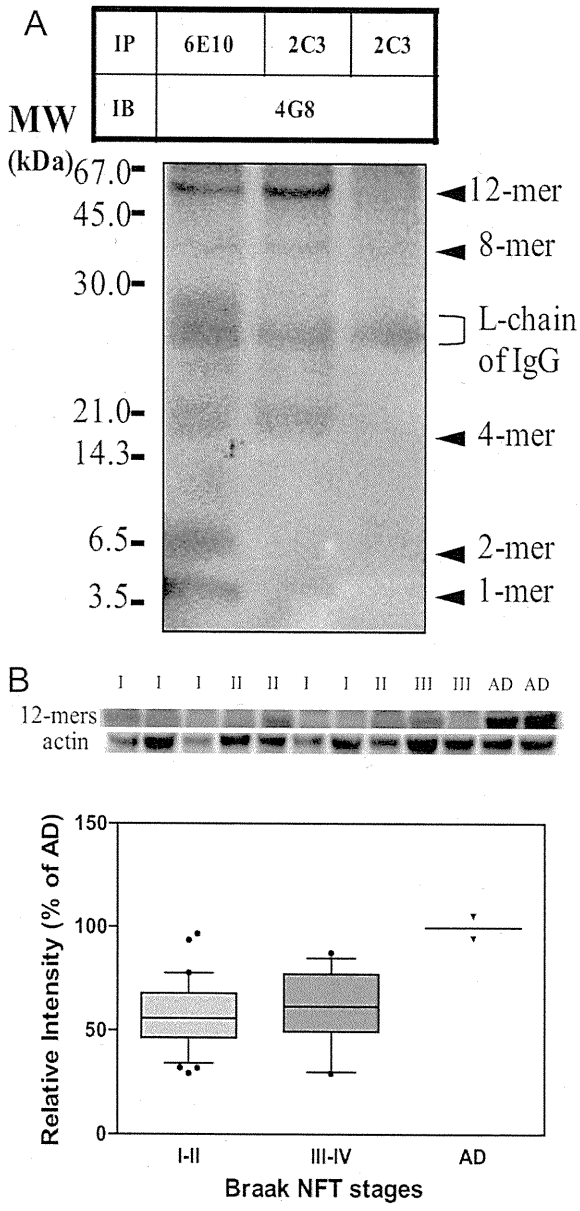

Fig. 1. Soluble oligomeric 2C3 conformers exist in human brain. **A**: 4G8 immunodetection of 6E10 or 2C3 immunoprecipitates in saline-soluble AD brain (lanes 1, 2) and control brain (lane 3). **B**: Relative intensity (percentage AD) of soluble 2C3-immunoreactive 12-mer in human entorhinal cortices obtained from 50 autopsy cases from the general aged population (Braak NFT stages I–II, n = 35; Braak NFT stages III–IV, n = 13, Braak NFT stages > IV, AD cases, n = 2).

were obtained from two AD individuals, 35 individuals with Braak NFT stages I–II, and 13 individuals with Braak NFT stages III–IV. As depicted in Figure 1B, approximately 45% and 60% levels of 12-mer (AD cases,

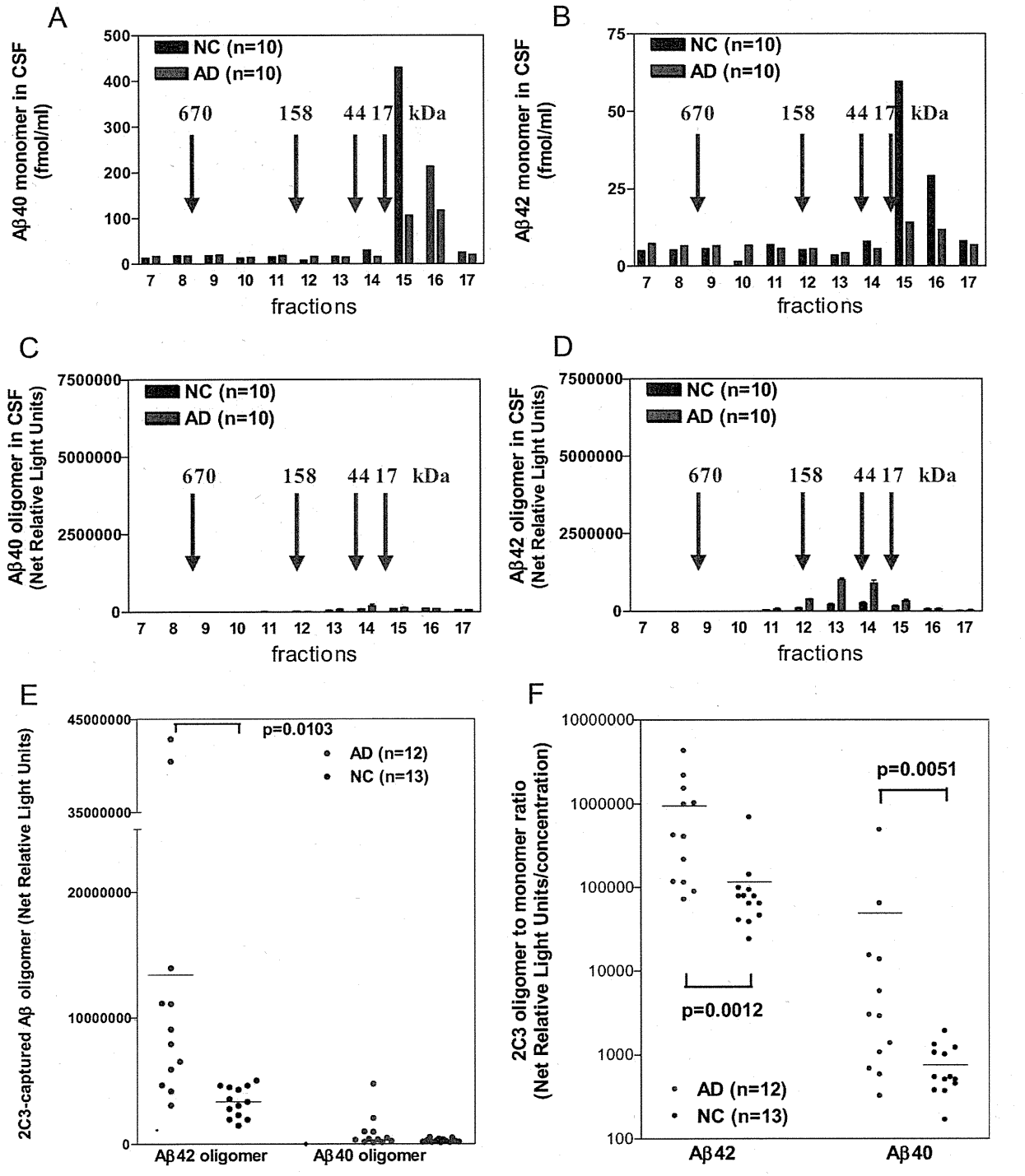

Fig. 2. Characterization of soluble oligomeric 2C3 conformers in human CSF. The presence of AβMs was analyzed by size-exclusion chromatography (SEC) using pooled whole CSF (A,B): $Aβ_{x–40}$ monomers (**A**) vs. $Aβ_{x–42}$ monomers (**B**). The presence of AβOs was analyzed by SEC using pooled lipoprotein-depleted CSF (C,D): $Aβ_{x–40}$ oligomers (**C**) vs. $Aβ_{x–42}$ oligomers (**D**). **E**: Quantitation of oligomeric 2C3 conformers measured in 12 AD patients (red circles) and 13 NC subjects (blue circles). **F**: $Aβ_{42}$ O/M index vs. $Aβ_{40}$ O/M index. Horizontal bars indicate the mean values. The statistical significance in comparison with the age-matched control group was analyzed by the Mann-Whitney test.

100%) had already accumulated in the ECs from NCs (Braak NFT stages I–II) and in those with mild cognitive impairment (Braak stages III–IV), respectively, suggesting that the accumulation of 12-mer precedes the appearance of cognitive impairment and increases as the Braak NFT stages progress. These findings clearly showed that the ECs of AD patients exhibit metabolic conditions that accelerate Aβ assembly.

To assess further the disease-related metabolic conditions, we focused on CSF, which mimics CNS environments. By a novel 2C3-based ELISA specific for sAβOs and BNT77-based ELISAs specific for sAβMs (Enya et al., 1999; Funato et al., 1999), we directly evaluated the disease-related metabolic conditions in CSF. To investigate the presence of native sAβOs, pooled, native, whole CSF (Fig. 2A,B) and pooled lipoprotein-depleted CSF (Fig. 2C,D) were subjected to SEC. Total cholesterol was detected in whole CSF fractions 7–14, indicative of lipoprotein-associated fractions. BNT77-based ELISAs revealed that the levels of lipoprotein-associated AβMs (fractions 7–14) in AD were similar to normal control levels (Fig. 2A,B), whereas the levels of lipoprotein-free $Aβ_{x-40}$ monomers (Fig. 2A) and $Aβ_{x-42}$ monomers (Fig. 2B) in native whole CSF were lower in AD than in age-matched normal controls. In contrast, ELISA of the oligomeric 2C3 conformer in pooled, lipoprotein-depleted CSF revealed the presence of larger Aβ species in fractions 12–15 with molecular masses ranging from 17 to 158 kDa, corresponding to 4- to-35-mers (Fig. 2C,D). The levels of the oligomeric 2C3 conformer in each fraction appeared to be higher in AD patients than in normal controls. To assess further the pathological relevance of this finding, the oligomeric 2C3 conformer was measured in 12 AD patients and 13 NCs. To address the issue on the presence of any metabolic conditions favoring Aβ assembly, AβMs were also measured to evaluate the AβOs/AβMs ratio (the O/M index). Interestingly, the levels of oligomeric 2C3 conformers composed of $Aβ_{42}$, not $Aβ_{40}$, are significantly higher in AD patients than in NCs ($P = 0.0103$; Fig. 1E). Noticeably, the O/M index for either $Aβ_{42}$ or $Aβ_{40}$ is significantly higher in AD patients than in NCs: $Aβ_{42}$ O/M index ($P = 0.0012$) vs. $Aβ_{40}$ O/M index ($P = 0.0051$; Fig. 1F). Recently, Fukumoto et al. (2010) reported a similar finding, supporting the reliability of our finding. Another group also reported that the levels of AβOs in CSF are significantly higher in AD patients than in NCs (Georganopoulou et al., 2005). Along with our findings, it is likely that the conversion of lipoprotein-free monomeric soluble Aβ into oligomeric assembly preferentially occurs in AD CSF, mirroring the disease-related metabolic conditions in the brain parenchyma. In support of our findings, a similar AD-related environmental alteration in CSF has been suggested (Ikeda et al., 2010). In contrast, it has been hypothesized that lower CSF $Aβ_{42}$ levels in AD patients can be ascribed to sequestration of soluble $Aβ_{42}$ into amyloid plaques. Several lines of evidence support this hypothesis; for example, an inverse correlation was found between CSF $Aβ_{42}$ levels and brain amyloid burden as evaluated by Pittsburgh compound B (PIB)-PET imaging (Klunk et al., 2004; Fagan et al., 2006). We have clarified this issue by comparing the levels of lipoprotein-free sAβMs in lipoprotein-depleted CSF from the 12 sporadic AD patients and 13 NCs. In the case of whole CSF, the relative amounts of sAβMs were similar in both groups (Fig. 3A). The LPD-CSF total AβM

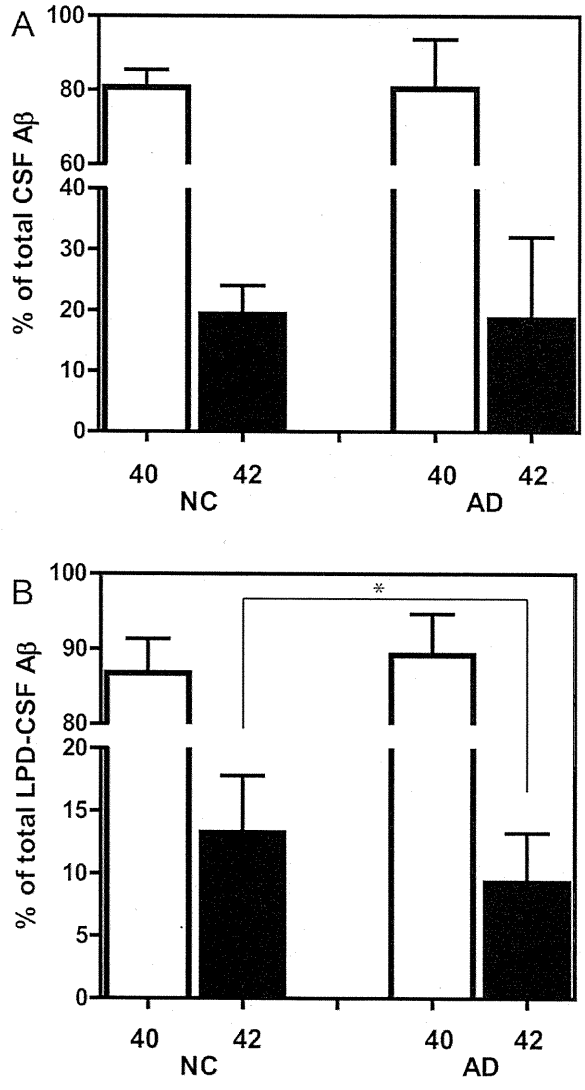

Fig. 3. Quantitation of $Aβ_{40}$ and $Aβ_{42}$ in native and lipoprotein-depleted CSF. The relative amounts (mean ± SD expressed as the percentage of total Aβ) of $Aβ_{40}$ (open bars) and $Aβ_{42}$ (solid bars) were quantitated in whole CSF (**A**) and lipoprotein-depleted CSF (**B**) in age-matched controls (NCs) and patients with sporadic Alzheimer's disease (AD). The levels of soluble Aβ species were measured by BNT-77-BA27 or BNT77-BC05 ELISA as described in Materials and Methods. Student's unpaired *t*-test revealed a statistically significant reduction (*$P = 0.0305$) in the relative amount of lipoprotein-free $Aβ_{42}$ in sporadic AD patients.

levels in both groups were relatively constant (302.8 ± 203.1 fmol/ml in sporadic AD patients and 463.9 ± 332.4 fmol/ml in NCs). In relative terms, the LPD-CSF AβMs values represented 31.6% ± 20.7% of the total Aβ in sporadic AD patients and 32.2% ± 13.5% of the total AβMs in NCs. Although these relative amounts of total lipoprotein-associated sAβMs (~70%) vs. lipoprotein-free sAβMs (~30%) remained essentially unchanged in sporadic AD patients, the amount of lipoprotein-free $Aβ_{42}$ was significantly lower ($P = 0.0305$) in the sporadic AD patients (9.3% ± 3.9%) than in NCs (13.2% ± 4.5%; Fig. 3B), which is in accordance with our above-mentioned finding that the level of oligomeric 2C3 conformers composed of $Aβ_{42}$ was significantly elevated in AD patients ($P = 0.0103$; see Fig. 2E). Note that about 70% of CSF sAβMs are normally associated with lipoprotein particles, whereas ~90% of sAβMs that circulate in normal plasma are associated with lipoprotein particles (Matsubara et al., 1999). These findings clearly indicate that the CNS constitutes a risky environment in which the lipoprotein–sAβMs interaction is impaired, leading to Aβ assembly. From this point of view, a key molecule to maintain monomeric $sAβ_{42}$ metabolism in CNS appears to be HDL-like lipoprotein particles. A similar intracerebral sequestration of sAβMs by an anti-Aβ antibody has been proposed to prevent the accumulation of toxic Aβ assemblies (Yamada et al., 2009). In the case of HDL, a previous study showed that Aβ depositions is enhanced in PDAPP transgenic mice under conditions of markedly suppressed HDL (Wahrle et al., 2005), whereas Aβ depositions is inhibited in PDAPP transgenic mice under conditions of markedly overexpressed HDL (Wahrle et al., 2008). ApoE4-HDL shows less cholesterol exchange between lipid particles and the neuronal membrane compared with apoE3-HDL (Zou et al., 2002), leading to altered membrane functions, e.g., signal transduction, enzyme activities, ion channel properties, and conformation of sAβ peptides, which contribute to the disease-related metabolic conditions. In this sense, the dissociation of $sAβ_{42}$ from or the lack of association with HDL-like lipoprotein particles not only constitutes a potential mechanism to initiate and/or accelerate the cascade favoring $Aβ_{42}$ assembly in the brain, but also results in a reduced clearance of physiological lipoprotein-associated $sAβ_{42}$ peptides in the brain.

ACKNOWLEDGMENTS

We acknowledge Dr. Hui Sun for her participation in the early stages of this project.

REFERENCES

Chromy BA, Nowak RJ, Lambert MP, Viola KL, Chang L, Velasco PT, Jones BW, Fernandez SJ, Lacor PN, Horowitz P, Finch CE, Krafft GA, Klein WL. 2003. Self-assembly of $Aβ_{1-42}$ into globular neurotoxins. Biochemistry 42:12749–12760.

Cleary JP, Walsh DM, Hofmeister JJ, Shankar GM, Kuskowski MA, Selkoe DJ, Ashe KH. 2005. Natural oligomers of the amyloid-β protein specifically disrupt cognitive function. Nat Neurosci 8:79–84.

Enya M, Morishima-Kawashima M, Yoshimura M, Shinkai Y, Kusui K, Khan K, Games D, Schenk D, Sugihara S, Yamaguchi H, Ihara Y. 1999. Appearance of sodium dodecyl sulfate-stable amyloid beta-protein (Abeta) dimer in the cortex during aging. Am J Pathol 154:271–279.

Fagan AM, Mintun MA, Mach RH, Lee SY, Dence CS, Shah AR, LaRossa GN, Spinner ML, Klunk WE, Mathis CA, DeKosky ST, Morris JC, Holtzman DM. 2006. Inverse relation between in vivo amyloid imaging load and cerebrospinal fluid Abeta42 in humans. Ann Neurol 59:512–519.

Fukumoto H, Tokuda T, Kasai T, Ishigami N, Hidaka H, Kondo M, Allsop D, Nakagawa M. 2010. High-molecular-weight beta-amyloid oligomers are elevated in cerebrospinal fluid of Alzheimer patients. FASEB J 24:2716–2726.

Funato H, Enya M, Yoshimura M, Morishima-Kawashima M, Ihara Y. 1999. Presence of sodium dodecyl sulfate-stable amyloid beta-protein dimers in the hippocampus CA1 not exhibiting neurofibrillary tangle formation. Am J Pathol 155:23–28.

Georganopoulou DG, Chang L, Nam JM, Thaxton CS, Mufson EJ, Klein WL, Mirkin CA. 2005. Nanoparticle-based detection in cerebral spinal fluid of a soluble pathogenic biomarker for Alzheimer's disease. Proc Natl Acad Sci U S A 102:2273–2276.

Geula C, Wu CK, Saroff D, Lorenzo A, Yuan M, Yankner BA. 1998. Aging renders the brain vulnerable to amyloid beta-protein neurotoxicity. Nat Med 4:827–831.

Gong JS, Sawamura N, Zou K, Sakai J, Yanagisawa K, Michikawa M. 2002. Amyloid beta-protein affects cholesterol metabolism in cultured neurons: implications for pivotal role of cholesterol in the amyloid cascade. J Neurosci Res 70:438–446.

Gong Y, Chang L, Viola KL, Lacor PN, Lambert MP, Finch CE, Krafft GA, Klein WL. 2003. Alzheimer's disease-affected brain: presence of oligomeric Aβ ligands (ADDLs) suggests a molecular basis for reversible memory loss. Proc Natl Acad Sci U S A 100:10417–10422.

Hass C, Selkoe DJ. 2007. Soluble protein oligomers in neurodegeneration: lessons from the Alzheimer's amyloid β-peptide. Nat Rev Mol Cell Biol 8:101–112.

Ikeda T, Ono K, Elashoff D, Condron MM, Noguchi-Shinohara M, Yoshita M, Teplow DB, Yamada M. 2010. Cerebrospinal fluid from Alzheimer's disease patients promotes amyloid beta-protein oligomerization. J Alzheimers Dis 21:81–86.

Katsuno T, Morishima-Kawashima M, Saito Y, Yamanouchi H, Ishiura S, Murayama S, Ihara Y. 2005. Independent accumulations of tau and amyloid beta-protein in the human entorhinal cortex. Neurology 64:687–692.

Kayed R, Pensalfini A, Margol L, Sokolov Y, Sarsoza F, Head E, Hall J, Glabe C. 2009. Annular protofibrils are a structurally and functionally distinct type of amyloid oligomer. J Biol Chem 284:4230–4237.

Klein WL, Krafft GA, Finch CE. 2001. Targeting small Abeta oligomers: the solution to an Alzheimer's disease conundrum? Trends Neurosci 24:219–224.

Klunk WE, Engler H, Nordberg A, Wang Y, Blomqvist G, Holt DP, Bergström M, Savitcheva I, Huang GF, Estrada S, Ausén B, Debnath ML, Barletta J, Price JC, Sandell J, Lopresti BJ, Wall A, Koivisto P, Antoni G, Mathis CA, Långström B. 2004. Imaging brain amyloid in Alzheimer's disease with Pittsburgh compound-B. Ann Neurol 55:306–319.

Koudinov AR, Koudinova NV, Kumar A, Beavis RC, Ghiso J. 1996. Biochemical characterization of Alzheimer's soluble amyloid beta protein in human cerebrospinal fluid: association with high density lipoproteins. Biochem Biophys Res Commun 223:592–597.

Lacor PN, Buniel MC, Chang L, Fernandez SJ, Gong Y, Viola KL, Lambert MP, Velasco PT, Bigio EH, Finch CE, Krafft GA, Klein WL. 2004. Synaptic targeting by Alzheimer's-related amyloid β oligomers. J Neurosci 24:10191–10200.

Lambert MP, Barlow AK, Chromy BA, Edwards C, Freed R, Liosatos M, Morgan TE, Rozovsky I, Trommer B, Viola KL, Wals P, Zhang C, Finch CE. 1998. Diffusible, nonfibrillar ligands derived from $A\beta_{1-42}$ are potent central nervous system neurotoxins. Proc Natl Acad Sci U S A 95:6448–6453.

Lashuel HA, Hartley D, Petre BM, Walz T, Lansbury PT Jr. 2002. Neurodegenerative disease: amyloid pores from pathogenic mutations. Nature 418:291.

Lesné S, Koh MT, Kotilinek L, Kayed R, Glabe CG, Yang A, Gallagher M, Ashe KH. 2006. A specific amyloid-beta protein assembly in the brain impairs memory. Nature 440:352–357.

Lin H, Bhatia R, Lal R. 2001. Amyloid beta protein forms ion channels: implications for Alzheimer's disease pathophysiology. FASEB J 15:2433–2444.

Matsubara E, Ghiso J, Frangione B, Amari M, Tomidokoro Y, Ikeda Y, Harigaya Y, Okamoto K, Shoji M. 1999. Lipoprotein-free amyloidogenic peptides in plasma are elevated in patients with sporadic Alzheimer's disease and Down's syndrome. Ann Neurol 45:537–541.

Matsubara E, Sekijima Y, Tokuda T, Urakami K, Amari M, Shizuka-Ikeda M, Tomidokoro Y, Ikeda M, Kawarabayashi T, Harigaya Y, Ikeda S, Murakami T, Abe K, Otomo E, Hirai S, Frangione B, Ghiso J, Shoji M. 2004. Soluble Abeta homeostasis in AD and DS: impairment of anti-amyloidogenic protection by lipoproteins. Neurobiol Aging 25:833–841.

Michikawa M, Gong JS, Fan QW, Sawamura N, Yanagisawa K. 2001. A novel action of alzheimer's amyloid beta-protein (Abeta): oligomeric Abeta promotes lipid release. J Neurosci 21:7226–7235.

Noguchi A, Matsumura S, Dezawa M, Tada M, Yanazawa M, Ito A, Akioka M, Kikuchi S, Sato M, Ideno S, Noda M, Fukunari A, Muramatsu S, Itokazu Y, Sato K, Takahashi H, Teplow DB, Nabeshima Y, Kakita A, Imahori K, Hoshi M. 2009. Isolation and characterization of patient-derived, toxic, high mass amyloid beta-protein (Abeta) assembly from Alzheimer disease brains. J Biol Chem 284:32895–32905.

Quist A, Doudevski I, Lin H, Azimova R, Ng D, Frangione B, Kagan B, Ghiso J, Lal R. 2005. Amyloid ion channels: a common structural link for protein-misfolding disease. Proc Natl Acad Sci U S A 102:10427–10432.

Schmechel DE, Saunders AM, Strittmatter WJ, Crain BJ, Hulette CM, Joo SH, Pericak-Vance MA, Goldgaber D, Roses AD. 1993. Increased amyloid beta-peptide deposition in cerebral cortex as a consequence of apolipoprotein E genotype in late-onset Alzheimer disease. Proc Natl Acad Sci U S A 90:9649–9653.

Selkoe DJ. 2002. Alzheimer's disease is a synaptic failure. Science 298:789–791.

Shankar GM, Li S, Mehta TH, Garcia-Munoz A, Shepardson NE, Smith I, Brett FM, Farrell MA, Rowan MJ, Lemere CA, Regan CM, Walsh DM, Sabatini BL, Selkoe DJ. 2008. Amyloid-betaprotein dimers isolated directly from Alzheimer's brains impairsynaptic plasticity and memory. Nat Med 14:837–842.

Tanzi RE, Bertram L. 2001. New frontiers in Alzheimer's disease genetics. Neuron 32:181–184.

Wahrle SE, Jiang H, Parsadanian M, Hartman RE, Bales KR, Paul SM, Holtzman DM. 2005. Deletion of Abca1 increases Abeta deposition in the PDAPP transgenic mouse model of Alzheimer disease. J Biol Chem 280:43236–43242.

Wahrle SE, Jiang H, Parsadanian M, Kim J, Li A, Knoten A, Jain S, Hirsch-Reinshagen V, Wellington CL, Bales KR, Paul SM, Holtzman DM. 2008. Overexpression of ABCA1 reduces amyloid deposition in the PDAPP mouse model of Alzheimer disease. J Clin Invest 118:671–682.

Walsh DM, Klyubin I, Fadeeva JV, Cullen WK, Anwyl R, Wolfe MS, Rowan MJ, Selkoe DJ. 2002. Naturally secreted oligomers of amyloid β protein potently inhibit hippocampal long-term potentiation in vivo. Nature 16:535–539.

Wellington CL. 2004. Cholesterol at the crossroads: Alzheimer's disease and lipid metabolism. Clin Genet 66:1–16.

Yamada K, Yabuki C, Seubert P, Schenk D, Hori Y, Ohtsuki S, Terasaki T, Hashimoto T, Iwatsubo T. 2009. Abeta immunotherapy: intracerebral sequestration of Abeta by an anti-Abeta monoclonal antibody 266 with high affinity to soluble Abeta. J Neurosci 29:11393–11398.

Zou K, Gong JS, Yanagisawa K, Michikawa M. 2002. A novel function of monomeric amyloid beta-protein serving as an antioxidant molecule against metal-induced oxidative damage. J Neurosci 22:4833–4841.

特集2　精神疾患モデル動物の妥当性

2. 変異 *Polg1* トランスジェニックマウスの双極性障害動物モデルとしての有用性

窪田　美恵*，加藤　忠史*

抄録：我々は，気分障害を伴う遺伝性ミトコンドリア病の原因遺伝子Polg1に点変異を持つマウス（変異 *Polg1* トランスジェニックマウス［mutant *Polg1* transgenic （Tg）マウス］）を作出し，双極性障害モデルマウスとしての妥当性を検討してきた。さらに，脳内遺伝子発現について，同腹野生型との差異を調べ，患者死後脳での遺伝子発現解析の結果と比較することにより，両者の共通点として，ミトコンドリア関連遺伝子である *Ppif* の発現減少を見出した。*Ppif* は，Ca^{2+}を制御する巨大チャネルであるPermeability Transition Pore（PTP）を調節する蛋白質，シクロフィリンD（cyclophilin D：CypD）をコードする。Tgマウス脳ミトコンドリアではCa^{2+}取り込みが亢進しており，この遺伝子発現減少がミトコンドリアにおけるCa^{2+}制御機能を変化させると考えられた。また，CypD阻害薬（NIM811）の慢性投与により，Tgマウスの輪回し行動における異常が抑制されたことから，CypDが新規治療薬の標的となる可能性がある。これらの結果から，Tgマウスのモデル動物としての有用性が示唆された。

日本生物学的精神医学会誌22（2）：109-116, 2011

Key words：bipolar disorder, mitochondrial DNA, polymerase γ, mitochondrial calcium uptake, cyclophilin D, NIM811

はじめに

我々は，双極性障害モデルマウスとして脳内にミトコンドリア機能障害を持つトランスジェニックマウスを作出した。このモデルマウスを作成する発端となった双極性障害におけるミトコンドリア機能障害についての所見や作成された動物において観察された行動異常については以前本誌に報告しているとおりである[20, 21]。本稿では，引き続きこのマウスで観察された行動表現型の基盤となる脳内異常を理解するために検討してきた研究結果について紹介したい。まず，同腹野生型と比較した際のモデルマウスでの脳内遺伝子発現変化について，さらに患者死後脳での遺伝子発現変化との共通点について検討し，その結果から得られた知見を元に行動薬理学的評価を行うことでこのマウスのモデル動物としての信頼性を確認した。

1．動物モデルの妥当性

動物モデルとして重要な条件として3つの満たすべき妥当性が提唱されている。まず，病因と同じメカニズムに基づいて作られているか，という構成概念妥当性，次に，モデルの示す行動変化が患者の病態に類似しているか，という表面妥当性，そして最後に，患者で効果の示されている薬剤がモデルにも類似した作用を示すかという，予測妥当性である。

これまで，これらを全て満たす双極性障害の動物モデルは存在しなかったと言って良かろう。既報の気分障害動物モデルは大きく4つのタイプに分類できる。

①薬理モデル：躁状態やうつ状態を薬理学的に再現したモデル
②遺伝モデル：過去に報告された疾患関連遺伝子を操作したマウス

Availability of neuron-specific mutant *Polg1* transgenic mice as animal model of bipolar disorder

＊独立行政法人 理化学研究所 脳科学総合研究センター 精神疾患動態研究チーム（〒351-0198　埼玉県和光市広沢2-1）Mie Kubota, Tadafumi Kato：Laboratory for Molecular Dynamics of Mental Disorders RIKEN Brain Science Institute, 2-1 Hirosawa, Wako, Saitama, 351-0198, Japan
【窪田　美恵　E-mail：tamie@brain.riken.jp】

③自然発症モデル：行動試験においてうつ状態を強く示す傾向をもつ系統を利用したモデル
④薬剤標的分子モデル：リチウムやバルプロ酸など気分障害の治療薬の作用点として考えられてきた分子に注目し，それらの役割を研究する目的で作出されたマウス

実際には，主に躁またはうつ状態のどちらかの表現型を示すモデルが提唱されており，双極性障害そのものを再現できるモデルの開発としては成功した例はほとんどないと思われる。

気分障害の中でも双極性障害における特徴は，うつ病に比較して遺伝的要因が大きく，躁とうつという2相性を示し，再発を繰り返すことである。我々の作成したマウスは，気分障害を伴う遺伝性ミトコンドリア病の遺伝子*Polg1*に点変異を持つマウス［変異*Polg1*トランスジェニック（mutant *Polg1* transgenic：m *Polg1* Tg）マウス］である。これまでに報告されてきた患者の脳画像解析によるエネルギーレベルの異常やミトコンドリアDNA多型など遺伝学的研究から，モデルとしての構成概念妥当性を満たすと考えている。そして，このm *Polg1* Tgマウスの長期的な輪回し行動測定において観察された周期的な行動変化や昼夜の行動パターンの異常などから表面妥当性も満たされたと考えられた。さらに予測妥当性に関して，双極性障害患者の治療薬反応性は，代表的な気分安定薬であるリチウムの他，バルプロ酸，ラモトリギン，オランザピンなどが奏効することが報告されている。また，うつ病には効果の認められている三環系抗うつ薬を双極性障害患者におけるうつ状態に対して投与することにより，躁転など症状の悪化が見られる特徴がある。以前に報告したように，このm *Polg1* Tgマウスで観察された輪回し行動異常に，リチウムや電気けいれん療法が奏効することから，予測妥当性が示されたと考えられた。特に，三環系抗うつ薬に対する反応については，アミトリプチリン200 mg/Lを10日間連続的に飲水投与したところ，m *Polg1* Tgマウスの中には夜間の行動量が投与後から突然増加し，薬物投与を止めた後にも，数週間その増加が持続した例が観察された。昼夜の異常な行動リズムも悪化する傾向が見られ，双極性障害患者のうつ症状に関して報告されている，躁転や急速交代型への移行に類似した行動変化がみられ，モデルとしての妥当性が支持された。

これらの結果からこのm *Polg1* Tgマウスは3つの妥当性を満たすモデルとして利用できると思われた。*POLG1*遺伝子は遺伝性ミトコンドリア病である慢性進行性外眼筋麻痺の原因遺伝子であり，この疾患を呈する患者では気分障害を合併することが多く報告されている。その一方，すべての双極性障害の患者は*POLG1*遺伝子に変異を持つわけではなく，一部の群で観察されるということも事実である。それでもミトコンドリアDNA異常を持つマウスで双極性障害と似たような行動異常，また細胞内シグナリング異常が見られるかどうかを検討することで双極性障害における共通の分子異常を解明できる可能性を考えた。共通の症状を引き起こすなんらかの生物学的基礎が存在し，同様の症状を引き起こすのであれば，その共通した病態生理のメカニズムを知ることによって最終的には病理学的異常を理解することができ，その症状を改善するための標的分子や薬剤が新規に開発できる可能性が考えられる。

2．m *Polg1* Tgマウス脳内遺伝子発現変化

そこで，m *Polg1* Tgマウス脳内における遺伝子発現変化を観察した。5ペアの同腹マウスの海馬，前頭葉を測定対象とし，Affymetrix社のマウス用DNAマイクロアレイを用いて両組織において発現変化を示す遺伝子群を同定した。発現が認められた約20,000個の遺伝子のうち，野生型に比較してm *Polg1* Tgマウスでは，前頭葉で1,471個，海馬で922個の遺伝子発現レベルに有意な違いが見られた。二つの領域で60遺伝子が共通しており，そのうち33遺伝子が同方向に変化していた。さらに33遺伝子のうち，18遺伝子が共通に発現低下を示し（**表1**），このうち，海馬において最も有意に変化していた遺伝子はグルココルチコイド受容体をコードする遺伝子*Nuclear receptor subfamily 3, group C, member 1*（*NR3C1*）だった。*NR3C1*は，両領域で野生型マウス脳内に比較して有意に発現レベルが低下しており，海馬では定量的PCR法による測定でも有意に低下していることが確認された（$p < 0.001$）。グルココルチコイド受容体の発現変化は他のうつ症状的表現型を示す動物モデルにおいても報告があり，うつ状態やストレス反応性に関連すると考えられている[1, 9, 12]。この結果もm *Polg1* Tgマウスの気分障害モデルとしての妥当性を支持する。また，15遺伝子が発現上昇し（**表2**），最も有意に変化していたのはスプライシングファクターの一つである*Sfpq*という遺伝子だった。興味深いことに*SFPQ*遺伝子発現レベルの変化は，双極性障害患者死後脳を用いた他の研究チームでのDNAマイクロ

表1　m *Polg1* Tg マウスの海馬，前頭葉において同腹野生型マウスに対して有意に発現レベルが低下していた遺伝子リスト

		Hippocampus		Frontal cortex			
Symbol	Gene title	Fold	p value*	Fold	p value*	Public ID	Probe set ID
Nr3c1	Nuclear receptor subfamily 3, group C, member 1	-1.12	< 0.001	-1.33	0.035	NM_008173	1421866_at
Ero1l	ERO（endoplasmic reticulum oxidoreductin）1-like（S. cerevisiae）	-1.08	0.001	-1.21	0.043	BM234652	1419029_at
Med26	Mediator complex subunit 26	-1.46	0.005	-1.62	0.007	AK017726	1452282_at
Npdc1	Neural proliferation, differentiation and control gene 1	-1.12	0.008	-1.12	0.028	NM_009849	1418259_a_at
2900052N01Rik	RIKEN cDNA 2900052N01 gene	-1.36	0.009	-1.32	0.026	AU067665	1436231_at
Kif5c	Kinesin family member 5C	-1.32	0.009	-1.50	0.047	AI844677	1450804_at
Flnb	Filamin, beta	-1.15	0.016	-1.29	0.002	AW538200	1426750_at
Rapgef6	rap guanine nucleotide exchange factor（GEF）6	-1.10	0.017	-1.11	0.038	BQ177183	1427412_s_at
Usp31	Ubiquitin specific peptidase 31	-1.09	0.017	-1.19	0.038	BM227490	1442099_at
Prmt3	Protein arginine N-methyltransferase 3	-1.21	0.020	-1.24	0.005	AK008118	1431768_a_at
Aif1l	Allograft inflammatory factor 1-like	-1.22	0.035	-1.07	0.016	BC024599	1424263_at
Cntn3	Contactin 3	-1.09	0.036	-1.13	0.024	NM_008779	1420739_at
Ppif	Peptidylprolyl isomerase F（cyclophilin F）	-1.12	0.038	-1.18	0.008	NM_134084	1416940_at
Copg	Coatomer protein complex, subunit gamma	-1.16	0.044	-1.13	0.009	BC024686	1415670_at
Enoph1	Enolase-phosphatase 1	-1.10	0.044	-1.28	0.002	BC021429	1423705_at
Smad3	MAD homolog 3（Drosophila）	-1.25	0.045	-1.28	0.019	BI150236	1450472_s_at
BC003266	cDNA sequence BC003266	-1.04	0.049	-1.08	0.039	NM_030252	1449189_at
Glud1	Glutamate dehydrogenase 1	-1.10	0.049	-1.19	0.040	BI329832	1416209_at

＊ Paired t test（< 0.05）.

表2　m *Polg1* Tg マウスの海馬，前頭葉において同腹野生型マウスに対して有意に発現レベルが上昇していた遺伝子リスト

		Hippocampus		Frontal cortex			
Symbol	Gene title	Fold	p value*	Fold	p value*	Public ID	Probe set ID
Sfpq	Splicing factor proline/glutamine rich（polypyrimidine tract binding protein associated）	1.26	0.003	1.27	0.039	BG061796	1439058_at
Erdr1 protein	Clone IMAGE：3983821	2.12	0.005	1.98	0.022	BC021831	1427820_at
Top1mt	DNA topoisomerase 1, mitochondrial	1.13	0.005	1.19	0.002	AF362952	1460370_at
Zc3h13	Zinc finger CCCH type containing 13	1.18	0.006	1.18	0.031	AW536655	1434894_at
Pspc1	Paraspeckle protein 1	1.37	0.013	1.27	0.009	BB590675	1423192_at
Hist2h2aa1	Histone cluster 2, H2aa1	1.33	0.032	1.48	0.024	BC010564	1418367_x_at
ImmP2l	Mitochondrial inner membrane protease subunit 2（IMP2-like protein）.	1.38	0.039	1.27	0.029	BB291417	1458099_at
EG633640	Predicted gene, EG633640	1.28	0.039	1.12	0.040	BG068672	1426607_at
Slc35e1	Solute carrier family 35, member E1	1.20	0.041	1.21	0.038	BB041864	1434103_at
Ube3c	Ubiquitin protein ligase E3C	1.22	0.041	1.29	0.019	BE690666	1444562_at
Rbm25	RNA binding motif protein 25	1.18	0.042	1.31	0.024	AI159652	1437862_at
Ptprn2	Protein tyrosine phosphatase, receptor type, N polypeptide 2	1.16	0.045	1.45	0.009	U57345	1425724_at
Polg	Polymerase（DNA directed）, gamma	1.42	0.045	1.23	0.007	BG064799	1423272_at
4930447A16Rik	RIKEN cDNA 4930447A16 gene	1.28	0.046	1.35	0.027	BB012182	1431671_at
Tradd	TNFRSF1A-associated via death domain	1.20	0.047	1.39	0.050	AA201054	1452622_a_at

＊ Paired t test（< 0.05）.

アレイを用いた遺伝子発現解析結果によっても報告されている[16]。また，Le-Niculescu らはDBP（D-box binding protein）ノックアウトマウスでの遺伝子発現解析結果から *Sfpq* 遺伝子発現変化について双極性障害における関連を提唱している[15]。

3．患者死後脳と m *Polg1* Tg マウス脳内遺伝子発現変化における共通点

双極性障害の病態に関連する神経学的基盤を探索するため，m *Polg1* Tg マウスの脳内遺伝子発現変化を利用し，以前に報告したヒト死後脳サンプルで

の遺伝子発現解析結果との共通点を検討した。患者サンプルでも共通に変化している所見がみつかれば，モデルマウスの表現型と患者の病態に共通に関連する分子の候補となりえると考えられるからである。次にm *Polg1* Tgマウス脳内で野生型に比較して発現変化していた遺伝子について双極性患者死後脳での発現レベルを確認した。

まず，m *Polg1* Tgマウス海馬と前頭葉で発現レベルが同方向に変動していた遺伝子についてヒトサンプルで検索できるようにするため，マウス用プローブ番号をヒトプローブ番号に変換したところ，ヒトでは39遺伝子に相当していた。そのリストを元に，スタンレー財団から提供された健常者と双極性障害患者の前頭葉（BA46）を用いて調べられた遺伝子発現解析結果に基づき，発現量の比較を行った。ヒト死後脳サンプルではサンプルpHが低いと遺伝子発現パターンが大きく変動することが報告されているため[10]，pHの影響があると思われるサンプルを除外し，健常群25例，患者群18例を用いて検討した。健常者に比べ，患者において発現レベルが有意に変化していた遺伝子は3プローブあり，*Ppif*，*Sfpq*の2つの遺伝子をコードしていた。どちらの遺伝子も発現レベルはm *Polg1* Tgマウスと同方向に変動していた（表3）。*Sfpq*についてはもともと4つの異なるプローブがマイクロアレイ上に存在し，発現レベル変化の方向にばらつきがあったこと，また*Ppif*発現レベルについては，特に2つのプローブで有意な差が見られたと同時にミトコンドリア関連遺伝子であることから，我々は*Ppif*に注目した。必ずしも*POLG1*遺伝子変異を持たない患者群でもm *Polg1* Tgマウスと同様の結果が確認されたことから，この遺伝子発現変化は，双極性障害の病態に関連する変化であると考えられた。

4．*Ppif*発現減少とミトコンドリア機能

*Ppif*はシクロフィリンD（cyclophilin D：CypD）をコードする遺伝子である。CypDはミトコンドリアマトリックスに存在し，内膜側に存在する蛋白質に結合してpermeability transition pore（PTP）と呼ばれるチャネル開口に関与していることが提唱されており[19]，PTP開口はアポトーシスやネクローシスに関連するとされている[4]。ミトコンドリアにはCa^{2+}の取り込みと排出に関与するそれぞれ独立した輸送機構があり，細胞質内Ca^{2+}濃度が上昇すると急速にユニポーターが働き，Ca^{2+}をとりこむ能力を有する。逆にミトコンドリア内のCa^{2+}は，主にNa^{2+}/Ca^{2+}交換輸送系により排出されると考えられているが，Ca^{2+}濃度が過剰に上昇した際には，このPTPも短く開口し，ミトコンドリア内からCa^{2+}が放出される。ミトコンドリアは，このように小胞体とともに細胞内のマイクロドメインを形成して，精密に細胞内Ca^{2+}濃度を制御している。

双極性障害と細胞内Ca^{2+}動態異常との関連性を示す所見は，現在のところ，患者血小板や嗅神経細胞を用いた結果により，G蛋白共役受容体を介して細胞内シグナリングを活性化させた時の細胞内Ca^{2+}反応異常として示され[5, 6, 11, 14]，双極性障害の素因になっている可能性が示唆されている。

我々は，*Ppif*発現変化とミトコンドリア機能変化を確認するため，m *Polg1* Tgマウス脳から単離したミトコンドリアでCa^{2+}取り込み能を測定した。一定濃度のCa^{2+}をミトコンドリアが取り込む様子を図1に示す。m *Polg1* Tgマウス由来ミトコンドリアでは，野生型マウスの脳ミトコンドリアに比べ，ミトコンドリア外のCa^{2+}が，短い時間でCa^{2+}投与前の静止レベルに戻る傾向が観察された。免疫抑制薬として使用されている，シクロスポリンAはCypD阻害薬であり，シクロスポリンA存在下でPTP開口を抑制することが示されている[7]ことからも，m *Polg1* Tgマウスミトコンドリアではptpに関与するCypD発現低下により，PTP開口が抑制されたと考えられた。

表3　m *Polg1* Tgマウスと双極性障害患者死後脳において共通に発現レベルが変化していた遺伝子リスト

		pH ≧ 6.5 samples (bipolar n = 18, control n = 25)		All samples (bipolar n = 33, control n = 34)				
Symbol	Gene title	Fold change	p value*	Fold change	p value*	Public ID	Probe set ID	Locus
PPIF	Peptidylprolyl isomerase F	-1.20	0.016	-1.19	0.005	NM_005729	201490_s_at	10q22-q23
PPIF	Peptidylprolyl isomerase F	-1.17	0.042	-1.11	0.095	BC005020	201489_at	10q22-q23
SFPQ	Splicing factor proline/glutamine-rich (polypyrimidine tract binding protein associated)	1.33	0.002	1.10	0.215	AV705803	221768_at	1p34.2

* t test（< 0.05）.

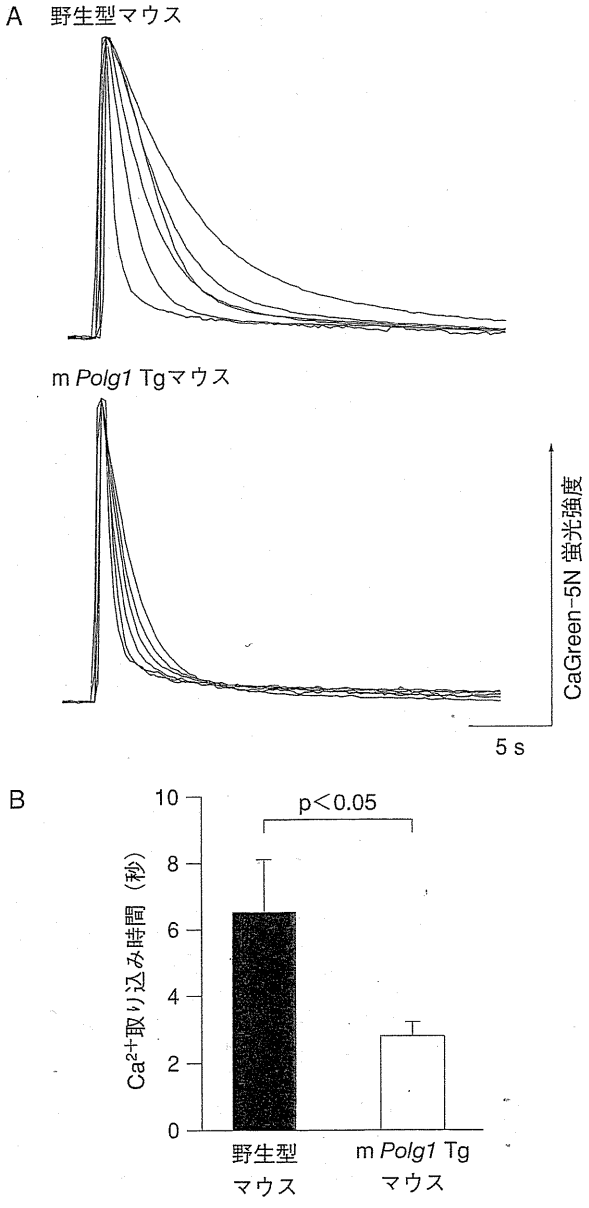

図1　m *Polg1* Tgマウス脳ミトコンドリアにおけるカルシウム取り込みの亢進

A　Ca^{2+}の濃度変化に対応して外液のCa^{2+}指示薬の蛍光強度が変化した様子。皮質・海馬を含む前脳からミトコンドリアを密度勾配法で単離し，蛍光色素である25 nM Calcium Green-5Nを含む緩衝液にインキュベーションした。ミトコンドリア呼吸基質として20 mMグルタミン酸2 mMマレイン酸を添加した。ミトコンドリア外液の蛍光強度（Ex488 nm，Em530 nm)を測定しながら，既知濃度のCa^{2+}液（100 nmol/mgミトコンドリア蛋白量）を添加した。一過性に上昇した外液内Ca^{2+}レベルがミトコンドリアによる取り込みにより徐々に減少した。同腹野生型マウス由来のミトコンドリアはCa^{2+}添加前のレベルにゆっくりと戻るのに比べ，m *Polg1* Tgマウス由来のミトコンドリアは急速に取り込む様子が観察された。

B　Ca^{2+}の取り込み時間。Ca^{2+}添加後のピークから添加前のレベルに戻るまでの50%減衰時間を6例で平均し，比較した。

5．シクロフィリンD阻害薬のm *Polg1* Tgマウス行動異常に対する作用

さらにCypD阻害薬を用いてm *Polg1* Tgマウスの行動異常に対する作用を観察した。免疫抑制剤として臨床的に使用されているシクロスポリンAは，ミトコンドリアではPTP開口を阻害することが知られている。これは，真菌Tolypocladium inflatum Gams種の代謝産物として産生される天然化合物であり，11個のアミノ酸よりなる環状ポリペプチドである。この免疫抑制活性は，細胞質のカルシニューリンへの作用によるものである。ポリペプチドの一部を改変することにより，カルシニューリンに対する作用を失わせ，ミトコンドリアCypD阻害作用のみを持つようにした誘導体として，NIM811が開発されている[8, 18]。我々は，単離ミトコンドリアを用いた*in vitro*実験で，NIM811がシクロスポリンAに比較してより低濃度でPTP開口を抑制することを確認した。

NIM811を投与したラットの脳では，虚血耐性を獲得できることが示されている[13]。気分安定薬であるリチウム投与後のラット脳も虚血耐性を示すことから[2, 3, 17]，NIM811もリチウム同様の気分安定効果を持ち，m *Polg1* Tgマウスで観察された双極性障害に類似した異常行動が抑制されるのではないかと仮定した。

そこで，2週間のNIM811慢性投与によるm *Polg1* Tgマウス異常行動への作用を確認した。m *Polg1* Tgマウスで報告されている特徴的な輪回し行動異常は，暗期から明期に切り替わった後の3時間程度の時間帯に，輪回し量が多く観察されるというものである。そこで，NIM811をm *Polg1* Tgマウスの腹腔内に40 mg/kg/dayで投与し，この輪回し行動量の異常に注目して観察を続けたところ，m *Polg1* Tgマウスの明期開始後3時間における輪回し行動量は，薬物投与前に比べ有意に抑制された（図2)。この結果から，CypD阻害薬は双極性障害において治療的意義を持つ可能性が示唆されると共に，m *Polg1* Tgマウスが双極性障害の動物モデルとして，気分安定薬開発のための行動薬理学実験に用いることが可能であることが示唆された。これまで気分安定薬として汎用されているリチウムだけでなく，バルプロ酸や非定型抗精神病薬も神経細胞保護作用を示すことが示されている。小規模な治験で有効性が示唆されたウリジンやNアセチルシステインがミトコンドリア機能に保護的な効果を持つことと考え合わせると，CypD阻害薬も同様に気分安定

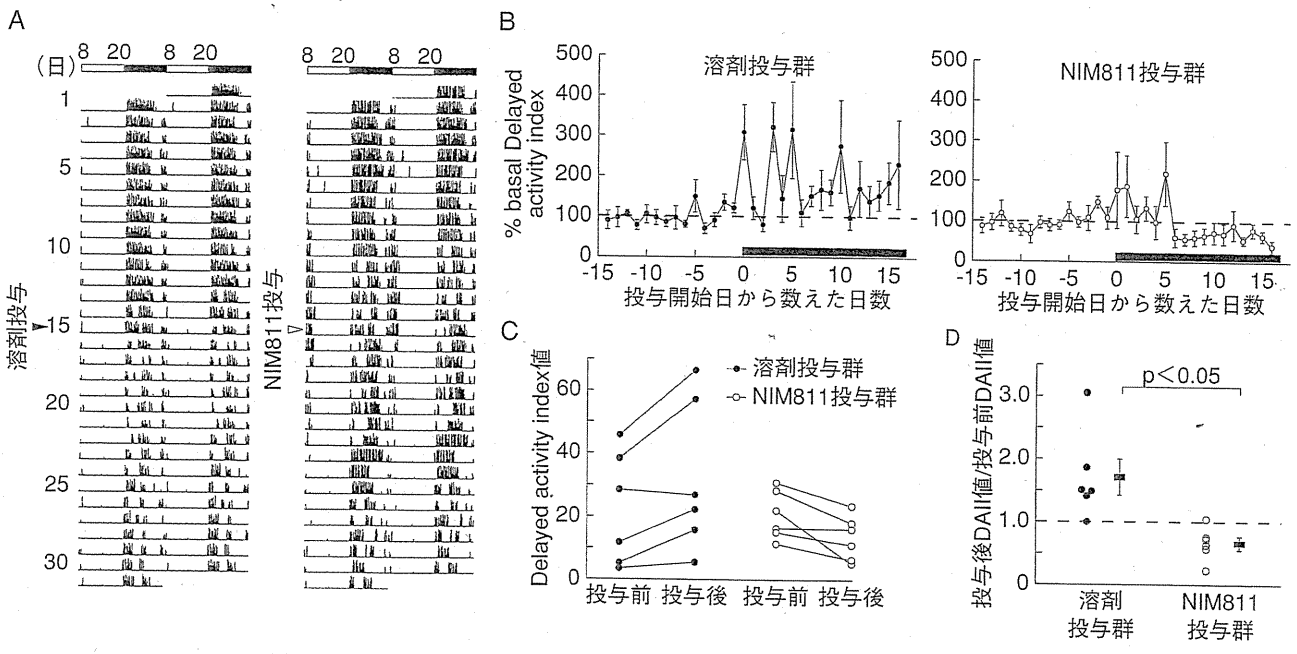

図2 m *Polg1* Tg マウスの輪回し行動異常に対する NIM811 慢性投与の効果

A 約4週間にわたる m *Polg1* Tg マウスの輪回し行動量をダブルプロットで示した。NIM811（40 mg/kg）および溶剤投与開始日を矢頭で示した（記録開始後15日目）。

B 投与開始前を基準とした輪回し行動異常の変化。明期開始後3時間の輪回し量を前日夜間（午後8時から次の日の午前8時まで）の輪回し総量で基準化し（基準値を点線で示した。），異常行動の指標（Delayed activity index，DAI）として測定した。同腹6匹分を1日ごとに平均し，NIM811および溶剤の投与開始日を原点として投与前14日間に対する，投与中16日間のDAI値の変化率をプロットした。

C NIM811および溶剤の投与前7日間と投与開始後10日目から16日目までの7日間のDAI値の平均（●：溶剤投与群，○：NIM811投与群）。

D 投与前に対する投与後のDAI値の比（●：溶剤投与群，○：NIM811投与群）。NIM811投与群では有意に抑制された（$p < 0.05$（Aspin-Welch's modified t test））。

薬としての候補になりえると思われる。このモデルマウスは，新たな作用機序を持つ双極性障害の治療薬の創薬研究や，気分安定薬の作用メカニズムを分子レベルで解明するための薬理学的研究に利用できると考えられる。

謝辞：本研究に使用したNIM811を提供していただいたノバルティスファーマ，ヒト死後脳サンプルを御提供いただいたスタンレー財団，および遺伝子発現解析に御協力いただいた東京大学精神科分子精神医学講座岩本和也准教授に感謝致します。

文　献

1）Boyle MP, Brewer JA, Funatsu M, et al (2005) Acquired deficit of forebrain glucocorticoid receptor produces depression-like changes in adrenal axis regulation and behavior. Proc Natl Acad Sci U S A, 102：473-478.

2）Chen G, Zeng WZ, Yuan PX, et al (1999) The mood-stabilizing agents lithium and valproate robustly increase the levels of the neuroprotective protein bcl-2 in the CNS. J Neurochem, 72：879-882.

3）Corson TW, Woo KK, Li PP, et al (2004) Cell-type specific regulation of calreticulin and Bcl-2 expression by mood stabilizer drugs. Eur Neuropsychopharmacol, 14：143-150.

4）Crompton M (1999) The mitochondrial permeability transition pore and its role in cell death. Biochem J, 341：233-249.

5）Dubovsky SL, Christiano J, Daniell LC, et al (1989) Increased platelet intracellular calcium concentration in patients with bipolar affective disorders. Arch Gen Psychiatry, 46：632-638.

6）Hahn CG, Gomez G, Restrepo D, et al (2005) Aberrant intracellular calcium signaling in olfactory neurons from patients with bipolar disorder. Am J Psychiatry, 162：616-618.

7）Hansson MJ, Persson T, Friberg H, et al (2003) Powerful cyclosporin inhibition of calcium-induced permeability transition in brain mitochondria. Brain Res, 960：99-111.